Synchrotron X-ray Studies of Metal-Based Drugs and Metabolites

R. C. ELDER* and MARLY K. EIDSNESS†

Biomedical Chemistry Research Center and Department of Chemistry, University of Cincinnati, Cincinnati, Ohio 45221-0172

Received March 24, 1987 (Revised Manuscript Received June 26, 1987)

Contents

Metal-based drugs have been in use for centuries. Gold-based drugs were apparently used by the Chinese as early as 2500 B.C.,[1] and colloidal gold was a cure-all of the middle ages. Tartar emetic (antimony potassium tartrate) has been used since 1600 in the treatment of parasitic disorders such as leishmaniasis and schistosomiasis[2] but is more frequently used in veterinary medicine than for humans. Mercury and its salts have been used to treat syphilis[3] whereas silver nitrate is applied topically to the eyes of newborns to prevent infection by gonococci.[4] The effects of these drugs have been discovered usually by accident, and it is only more recently that systematic, "scientific" studies of metal-based drugs have come to the fore. Since 1950, gold-based drugs have been shown to cause remission of rheumatoid arthritis,[5] a platinum-based drug has been shown to have a 95% cure rate for certain types of metastatic testicular cancer,[6] and a variety of technetium radiopharmaceuticals have been prepared to image selected organs for both diagnostic and prognostic medicine.[7]

Although these last three cases involving gold, platinum, and technetium drugs are of immense importance, chemical investigations of these drugs have proven difficult. Biologically relevant studies using animals or human patients are frequently stymied by the low concentrations of the drugs and the intractability of the biological matrix when a molecular understanding is desired. Model systems are more ammenable to classical chemical methods but may easily lack relevance. Clearly nonclassical techniques are needed, and real progress has come in adapting techniques of molecular biology,[8] new forms of chromatography,[9] electrochemistry,[10] and high-sensitivity NMR[11] to study metal-based drug biology. Another relatively new set of techniques showing considerable promise involves X-ray absorption spectroscopy (XAS) and X-ray scattering. A revised interpretation of extended X-ray absorption fine structure (EXAFS)[12] and development of high-intensity synchrotron X-ray sources using electron storage rings[13] have led to vastly increased interest in these techniques and led us and others to apply them in studies of metal-based drugs. We review here the work performed and results obtained with comments on the advantages and limitations of these X-ray techniques for medical research. Briefly, these are structure-determining tools that can be applied to nearly any sample: liquid solutions, solids, or tissues, for example. Element-specific information on oxidation state and electronic and geometric structure is obtained in a matter of hours for samples of moderately low concentration (millimolar or greater). In many circumstances relevant to medical or biological research these are the only structural tools that can be applied. We do not review the calculational methods by which structural information is extracted from EXAFS or scattering data nor the experimental techniques whereby the data are measured. Excellent reviews on these subjects are already in the literature.[14-16]

I. Gold Antiarthritic Drugs and Gold-Biological Complexes

The research field of gold biochemistry is relatively young. Interest in this area has grown since the efficacy of Au(I) for treatment of rheumatoid arthritis (RA) was

†Current address: School of Chemical Sciences, University of Georgia, Athens, GA 30602.

0009-2665/87/0787-1027$06.50/0

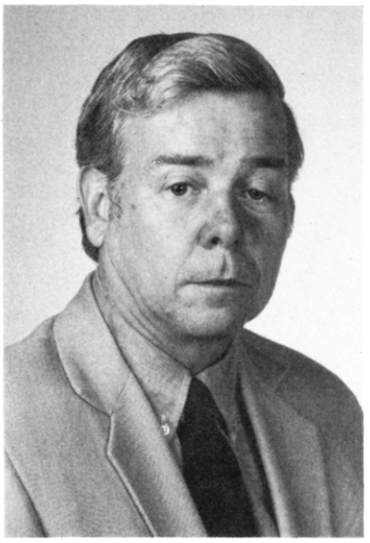

Richard C. Elder was born in Ann Arbor, MI, in 1939. He obtained the undergraduate degree of Honors B.S. in Chemistry in 1961 from St. Louis University. He completed his Ph.D. studies with Professor F. A. Cotton at the Massachusetts Institute of Technology in 1964. After a 1-year postdoctoral stint in Professor Cotton's laboratory at MIT, he was appointed Instructor and then Assistant Professor at the University of Chicago. He came to the University of Cincinnati in 1970 and was promoted to Full Professor in 1978. His research interests are centered on studies of metallodrugs and their metabolites as well as the development of new structural tools using synchrotron X-rays.

Marly K. Eidsness was born in Lake Preston, SD, in 1954. She obtained undergraduate degrees, B.F.A. (sculpture) in 1977 and B.A. in Chemistry in 1982, from California State University, Long Beach. She completed her Ph.D. studies in Physical Chemistry at the University of Cincinnati in 1984, working with R. C. Elder. After 1 year of joint postdoctoral work at Stanford University (Materials Science) and Exxon (Corporate Research Science Laboratories), she continued as a postdoctoral research associate with R. A. Scott in the School of Chemical Sciences at the University of Illinois, Urbana-Champaign, and is currently at the University of Georgia, Athens. Her research interests are in structural and functional studies of metalloproteins utilizing X-ray absorption and X-ray anomalous scattering methods.

established in 1961.[5] To date, Au(I) pharmaceuticals are the only class of drugs known to halt the progression of the disease. The therapeutic mode of action of gold remains largely unknown. Numerous in vitro experiments concerning the reactivity of gold with biologically relevant materials have been reported.[17,18] It is apparent from these studies that gold(I) preferentially

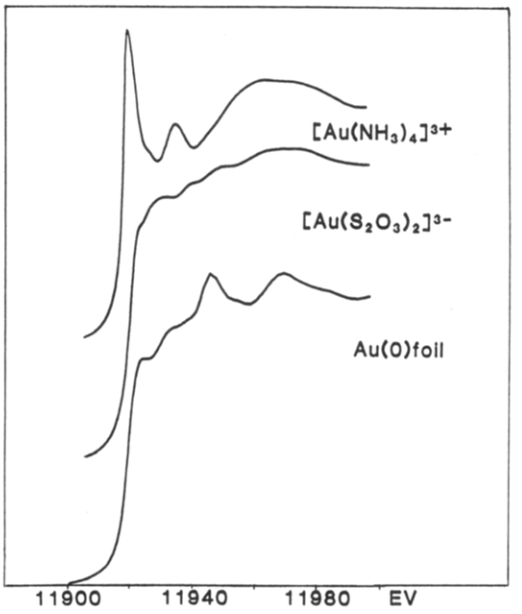

Figure 1. X-ray absorption near edge structure (XANES) showing the characteristic "white-line", 2p → 5d transition for gold(III) complexes and the two characteristic peaks in gold(0) metal XANES as well as the rather featureless gold(I) edge structure.

seeks sulfur binding sites. Various suggestions have been offered to explain the mode of action of the gold-based drugs. On the basis of observations of serum sulfhydryl levels, Lorber[19] suggested that gold(I) modifies the sulfhydryl (SH)–disulfide (S–S) exchange. Brown and Smith[20] have more recently elaborated on the possible role of gold–thiol interactions in the mode of action of the gold-based RA drugs. A possible mode of action may be the interaction of gold drugs with lysosomes, present in large numbers in RA patients. Lysosomes contain hydrolases, which upon release can destroy articular matter. Since it is known that gold therapy (chrysotherapy) leads to concentration of gold in lysosomes,[21] the inhibition of lysosomal hydrolases may be the result of the drug action.[22]

The fate of gold pharmaceuticals in vivo remains for the most part obscure. To learn more about the metabolic reactions of the gold drugs, experimental methods must be used that reveal information about the gold complexes that form as the drug is transported throughout the body. EXAFS and XANES spectroscopy are methods well suited for this. Probably the most important virtue of the X-ray absorption experiment is the freedom to examine samples in any form of matter. Samples of animal tissue, noncrystalline drugs, and gold–protein complexes have been routinely used in the antiarthritic gold drug study.

Our intention here is to present the structural information obtained wholly or in part from X-ray experiments. The details of the experiments and the methods of data analysis are not emphasized. Rather we relate the structural findings to their possible implications in rheumatoid arthritis research. We will attend to the strengths and weaknesses of these X-ray techniques as they apply to gold-biological studies.

A. Features of Au EXAFS and XANES Spectra

A description of some characteristic features of the Au L_{III} absorption edge spectrum will be useful for the

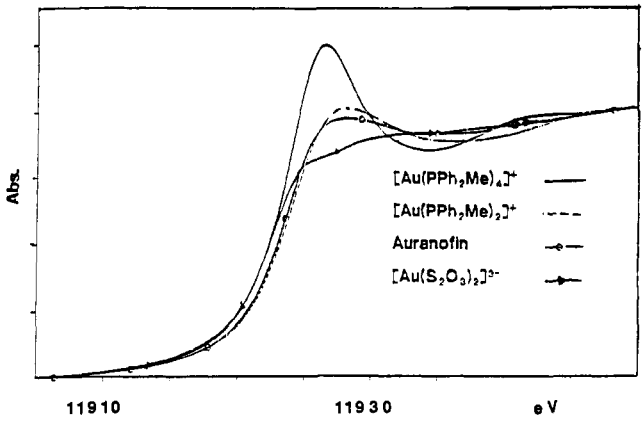

Figure 2. Superposition of the XANES from compounds with zero, one, two, and four Au–P bonds showing the characteristic Au–P hump increasing with Au–P coordination number. Auranofin is the generic name of the oral antiarthritis drug (triethylphosphine)gold(I) tetraacetylthioglucose.

interpretations of the gold spectra from biological materials discussed later. Beginning with the X-ray absorption near-edge structure (XANES) region of the spectrum, one can clearly identify the oxidation state of gold in a compound by the shape of the edge. The common oxidation states of gold, Au(0), Au(I), and Au(III), are easily distinguishable. Spectra from complexes with these three gold oxidation states are shown in Figure 1. Metallic gold is identified by two broad peaks in the edge region at 11.945 and 11.967 keV, and these two peaks are retained even when the gold metal particle size is as small as 10. Å in diameter. Spectra of Au(III) compounds show a sharp spike on the edge rise that may be assigned to a 2p → 5d transition, as Au(III) has an unfilled 5d subshell. The edge spectrum of Au(I) is rather featureless by comparison. Au(I) has a $5d^{10}$ configuration, and thus no transition to the 5d level is possible. This oxidation state can be identified with reasonable certainty[23] by eliminating the possibility of Au(0) and Au(III) oxidation states.

The assignment of the oxidation state of a gold compound can be made also by determining the inflection point of the edge rise. We have found that all of the Au(I) compounds we have measured have inflection points within the range of 11.922–11.924 keV (relative to the Au(0) inflection point at 11.9212 keV). Au(III) inflection points fall within the energies of 11.919–11.921 keV. It is clear that Au(III) oxidation states have inflection points at lower energies than Au(0) or Au(I). This opposes the expected trend of increasing inflection point energy with increasing oxidation state.[27] A possible explanation for this is that the edge feature of all Au(III) compounds is a bound-state transition that actually overlays the "true" inflection point expected for Au(III). Due to the distinctive qualitative features of Au(0), Au(I), and Au(III) edges, and the specific energy ranges of the inflection points of Au(I) and Au(III) spectra, the oxidation state of any biological gold complex may be readily determined.

We have observed that gold compounds with phosphorus ligands usually exhibit an edge-rise "fingerprint". This gold–phosphorus feature increases as the number of ligating phosphorus atoms increases. The phosphorus edge effect is illustrated in Figure 2. Of significance is the fact that no such spectral feature exists in any

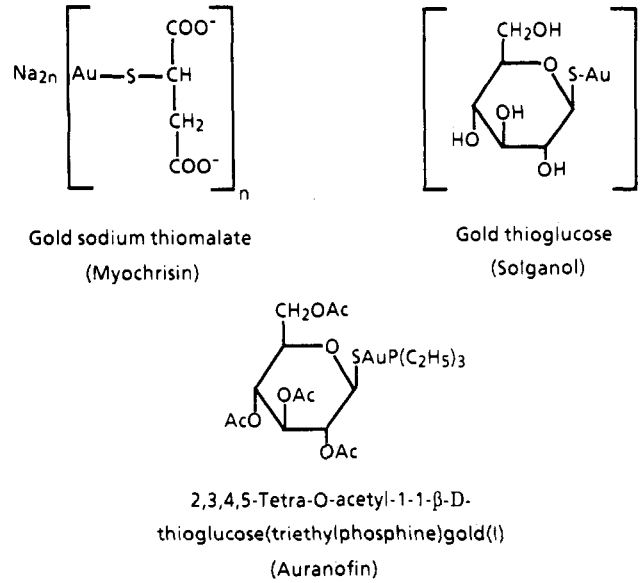

Figure 3. Chemical formulations of three gold-based antiarthritis drugs.

of the gold complexes that bind to sulfur but not phosphorus. Thus, phosphorus and sulfur scattering atoms can be distinguished by their XANES spectra. The EXAFS oscillations of phosphorus and sulfur are nearly identical. Since S or P atom identification cannot be made from EXAFS curve-fitting alone, this fortuitous means of distinction using XANES has proven to be of importance in the EXAFS curve-fitting analyses of complexes that might contain sulfur and/or phosphorus ligands.

Not only is EXAFS unable to discriminate between neighbors in the periodic table as back-scatterers, it fails, as well, to flag reliably metal–metal interactions. Initially we thought that gold–gold interactions would be observed in the EXAFS of polymeric gold-biological complexes. However, EXAFS measurements of several structures of known Au–Au distances showed that Au–Au fine structure was observed only when the distance was less than about 3.0 Å.[28] In fact, evidence of gold–gold bonds has not been observed in the EXAFS of any biological sample.

B. Antiarthritic Au(I) Drugs

The Au(I) pharmaceuticals currently approved for clinical use in the United States include sodiumgold(I) thiomalate (myochrisin) and gold(I) thioglucose (solganol). These drugs are administered by injection. A new oral drug [(triethylphosphine)(tetraacetylthioglucose)gold(I), auranofin] was recently approved for use in the United States and is in clinical use in many other countries as well. Figure 3 shows the structural formulas for these drugs. The crystal structure of the oral drug shows[29] gold linearly coordinated by the sulfur atom of the sugar and the phosphorus from triethylphosphine to give a discrete, monomeric molecular species. Since no one has successfully crystallized the injected drugs, the details of their structures have not been determined by single-crystal X-ray diffraction. Although the ligand to gold ratio for the injected drugs is about 1:1 based on stoichiometry, the preference for two-coordinate linear configurations in Au(I) chemistry makes a monocoordinate gold structure unlikely, and the structures of the drugs have been presumed to be

polymeric with bridging sulfur atoms.[30,31] EXAFS studies by Sadler et al.[32] and Elder et al.[27] provided the first direct evidence confirming the polymeric structure of these drugs.

Sadler and co-workers measured the Au L_{III} absorption edge in the compounds myochrisin, solganol, and $Na_3Au(S_2O_3)_2$, which served as a test compound. Bond lengths were determined from the Fourier transform of the data using calculated phase shifts. The gold to ligating sulfur distance in the thiosulfate complex was determined to be 2.33 Å which may be compared to the crystal structure value of 2.28 Å.[33] Analysis of myochrisin and solganol EXAFS data revealed an Au–S bond distance of 2.37 Å and a coordination number of 2.

We independently measured the EXAFS spectra at the Au L_{III} edge of myochrisin and solganol both as solids and in solution.[27] The curve-fitting analysis method[14] we used requires model compounds of known structure. For myochrisin and solganol structures the gold atoms were determined to be coordinated by 2.0 sulfur atoms in both cases with Au–S bond lengths of 2.30 and 2.31 Å, respectively. The errors in these calculations were estimated to be ±10% for the coordination number and ±0.01 Å in the bond distances, based on EXAFS structural determinations of several AuS-type compounds of known structures. EXAFS structural results from solutions of 0.015 M myochrisin and solganol yield 1.9 and 2.0 sulfur atoms with Au–S bond distances of 2.29 and 2.30 Å, respectively. Comparison of the EXAFS results for the solid drug samples and the solution samples indicate that the structures are essentially identical in both phases. Ideally, one would like to collect EXAFS data for the drug at its therapeutic concentration in the blood, which rarely exceeds 50 μM.[22] However, this concentration is too low for EXAFS experiments. The lower limit of detection in the fluorescence mode is generally about millimolar. The requirement for moderately high concentrations of the absorbing element is one of the limitations of EXAFS spectroscopy.

The discrepancy between the work of Sadler and our own seems more apparent than real. Using calculated phase shifts, Sadler is in disagreement with the bis(thiosulfato)gold(I) crystal structure by 0.05 Å. If this value is used to correct his drug distance calculations, the value of 2.32 Å results in close agreement with our values of 2.30 and 2.31 Å. It seems clear that no matter the methodology, both groups agree that gold has two sulfur neighbors at reasonable distances for Au–S bonding and that these results require an oligomeric or polymeric formulation for the drugs. Our X-ray scattering work, described at the end of this section confirms these results and provides further details of the structures of myochrisin and solganol.

C. Au–Albumin Complexes

Serum albumin is the principal carrier in blood for the intramuscularly injected drugs myochrisin and solganol. Following the administration of one of these Au(I) pharmaceuticals, 80–95% of the gold binds to serum albumin.[18] It was proposed by Gerber,[34] in 1964, that sodiumgold(I) thiomalate binds to the single, reduced sulfhydryl residue, cysteine-34 (Cys-34), of bovine serum albumin. He further suggested that the thiomalate ligand was retained upon complex formation. However, more recent work by Jellum and Munthe disputed this claim.[35] These authors suggested that the thiomalate ligand of the drug was displaced from gold when complexed with albumin. Clearly, the structural integrity of the drug in these reactions was not well established. EXAFS and XANES spectroscopy have been used to obtain some structural information about gold coordination in complexes that form in vitro between bovine serum albumin (BSA) and several gold compounds.

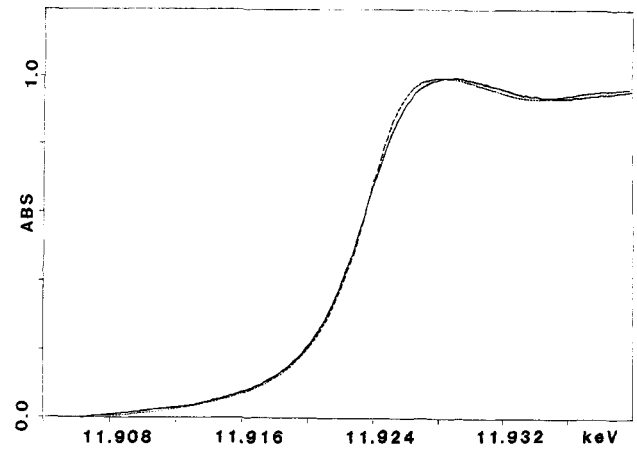

Figure 4. XANES spectra of auranofin (—) and auranofin bound to bovine serum albumin (BSA) (- - -), showing retention of the phosphine by gold on binding to BSA.

1. *Auranofin–BSA*

Auranofin has phosphorus and sulfur atoms bound to gold, and this oral drug can be shown to bind to BSA. Several binding modes are possible, and EXAFS/XANES spectroscopy has been used as part of an effort to sort them out.[36] Examination of the XANES spectrum reveals that gold has remained in the 1+ oxidation state, with the edge rise inflection point falling within the energy range expected for Au(I) compounds. The presence or absence of phosphorus ligation can be assessed by analysis of the XANES spectrum. As discussed in section IA, the shape of the edge spectrum for materials with gold–phosphorus bonds is unique. In Figure 4 the edge spectrum of auranofin–BSA is compared with that of auranofin. The similarity in these spectra indicates that indeed the gold–phosphorus bond is retained in the auranofin–BSA complex. Thus, from XANES it is possible to say that the bound gold in the auranofin–BSA complex has been neither oxidized nor reduced and that the gold–phosphorus bond of the drug has remained intact. This latter fact was also confirmed by ^{31}P NMR of the auranofin–BSA complex, which indicated the presence of the (triethylphosphine)gold moiety.[36]

EXAFS data were fit for sulfur and phosphorus coordination of gold, yielding 0.6 sulfur atom at 2.27 Å and 1.7 phosphorus atoms at 2.29 Å. These results may be compared to the EXAFS fit for auranofin itself: 1.1 Au–S at 2.25 Å; 1.0 Au–P at 2.32 Å. In both cases the Au–S and Au–P distances appear reversed compared to those in the crystal structure: Au–S, 2.29 Å; Au–P, 2.26 Å. This is further evidence of the difficulty of distinguishing sulfur and phosphorus in EXAFS curve fitting. Although gold binding by one sulfur and one phosphorus seems likely, the question remains where

on BSA does auranofin bind. The possibility of binding between the protein and the acetylated sugar moiety of intact auranofin seems remote since any binding of that type would be expected to be extremely weak. It appears most likely that this binding occurs after the thiosugar has been cleaved and the remaining (triethylphosphine)gold binds to the sulfhydryl of Cys-34 in BSA. The observation that only 60% of the BSA molecules have free sulfhydryl groups at Cys-34 (the others are blocked most likely by disulfide formation with additional cysteine present in the serum) and that the amount of auranofin bound agrees with free Cys-34 sulfhydryl content strongly implies Cys-34 binds the gold in auranofin. Additional support for binding via a thiolate exchange reaction comes from our observation that, analogously, (triethylphosphine)gold(I) thioglucose ("deacetylated auranofin") rapidly reacts with tetraacetylthioglucose to exchange thiosugars and re-form auranofin.[37]

2. Myochrisin–BSA

EXAFS and XANES spectroscopy, in tandem with other experimental techniques, have been used to probe the structure of the gold binding site in the complex that forms between myochrisin and bovine serum albumin.[38] The questions posed by the conflicting results of Gerber[34] and Jellum and Munthe[35] are resolved, on the basis of this study. Combining several experimental tools in a collaborative study with Professor C. F. Shaw's group at the University of Wisconsin—Milwaukee, we identified ligands binding to gold.

Our results indicate that there are two gold binding modes with albumin, dependent on the concentrations of albumin and gold(I) thiomalate. When albumin was present in excess, as would be the case in vivo during chrysotherapy, gold was found to bind exclusively to Cys-34. The Fourier transform of the EXAFS data from this sample shows a single peak consistent with a relatively symmetric arrangement of atoms. Curve-fitting results indicated that the gold coordination sphere consisted of 2.1 sulfur atoms at 2.30 Å. Sulfur ligation through Cys-34 of albumin was supported by electrophoretic measurements. If gold(I) thiomalate were to bind to any of the other sulfur atoms in albumin (thioethers or disulfides), the electrophoretic mobility of the complex would be expected to increase. This was not observed and therefore provided indirect evidence that the gold binding site on albumin is Cys-34. Also, the gold binding to albumin appears to saturate this site when the ratio of bound gold to unblocked sulfhydryl groups, vide supra, is 1:1.

The identity of the ligands attached to gold was further clarified by gel exclusion chromatography and ^{35}S radiotracer studies. The $Au–S_2$ configuration could conceivably arise from two albumin molecules bound to gold. In this case, the thiomalate ligand would no longer be bound to gold. Two albumins involved in complexation with gold would be expected to have a shorter retention on a gel column, compared to unreacted albumin. Experiments showed that there was essentially no change in the retention time of the complex. This eliminated the possibility of more than one albumin per complex. An experiment using ^{35}S–gold(I) thiomalate showed labeled sulfur and gold to be taken up in the complex in a 1:1 ratio. Summarizing, the complex formed from a reaction of excess albumin relative to gold(I) thiomalate was shown to occupy a single gold binding site on albumin. EXAFS analysis indicated that the gold coordination sphere consisted of two sulfur atoms at 2.30 Å. Several other experimental methods identified the ligands bound to gold as thiomalate and Cys-34.

A second, weaker binding in the complex was observed when the conditions of the reaction were such that the gold(I) thiomalate concentration greatly exceeded that of albumin. The EXAFS analysis of this complex revealed that the gold was coordinated by 2.0 sulfur atoms at a distance of 2.30 Å. This complex was known to have about seven gold atoms per unblocked Cys-34. A formulation that could accommodate multiple gold atoms in two-coordinate sulfur arrangements involves multiple gold(I) thiomalate units connected by bridging sulfur atoms. Since we have shown that myochrisin is polymeric in solution, the so-called weak binding site seems likely to result from binding the drug, in an oligomeric form, to the strong binding site, that is Cys-34.

These results can be related to chrysotherapy. The concentration of serum albumin in the body is on the order of 590 μM. During chrysotherapy, the concentration of Au in serum is less than 50 μM. The results from the myochrisin–albumin complex that formed when albumin was present in excess best approximates the in vivo condition. Thus, the probable structure of the myochrisin–albumin complex in vivo is (thiomalate) S–Au–S (Cys-34).

3. Et_3PAuCl–Sulfhydryl-Blocked BSA

Since the binding site in BSA was shown in the previous studies to be Cys-34, the question arose whether there are other binding sites for gold complexation with BSA. To examine other sites, we incubated a sulfhydryl-blocked form of BSA with Et_3PAuCl and studied the product by EXAFS and XANES. The XANES spectrum was used to determine whether the gold–phosphorus bond remained intact in Et_3PAuCl after treatment with blocked BSA. Interestingly, P–Au–Cl systems, such as Et_3PAuCl and Ph_3PAuCl, do not show evidence of the gold–phosphorus bond in their XANES spectra. However, the phosphorus edge effect is observed in the edge rise of $(Ph_3P)_2AuCl$ XANES. Comparison of the edge spectrum of the albumin–gold complex with that of Et_3PAuCl (Figure 5) shows that the phosphorus peak appears in the edge spectrum after complexation and is similar in magnitude to a one-phosphorus system (see Figure 2). This analysis implies that phosphorus remained bound to gold in the albumin complex. While we have not provided a theoretical basis for identifying gold–phosphorus binding by the XANES type peak, we have seen this peak in every Au–P compound we have studied with one exception and we have never seen this feature in any of the Au–S compounds with no phosphorus. The semiquantitative relation between peak height and number of phosphorus neighbors also encourages us to believe that the feature is a reliable marker for Au–P bonding. EXAFS curve fitting was used to determine the identity of the atoms in the immediate vicinity of gold. The somewhat askew shape of the Fourier transform peak indicated that different types of atoms might be bound to gold.

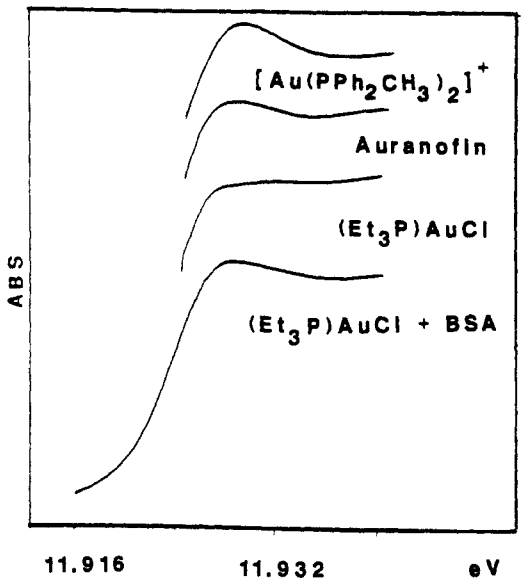

Figure 5. XANES spectra of $(Et_3P)AuCl$ bound to BSA, showing the characteristic Au–P edge feature.

Phosphorus and nitrogen (or oxygen) parameters were used to successfully fit the data. Bond lengths of 2.25 and 2.06 Å were calculated for 1.1 P and 1.1 N (or O), respectively.[36]

Only a tentative assignment of the P and N ligands can be made. Since albumin has no phosphorus-containing groups, the Au–P bond in the complex must derive from the triethylphosphine moiety. There are a number of possible binding sites for the Au–N coordination in BSA. There are a total of 17 histidine amino acid residues within albumin. Since EXAFS curve-fitting analysis cannot distinguish between nitrogen and oxygen atoms, the possibility that gold may be coordinated to oxygen, perhaps in carboxylate groups, must also be considered. The important observation here is that, if denied access to a thiolate sulfur, a phosphinogold(I) moiety will bind to a low-Z atom such as nitrogen or oxygen.

D. Myochrisin–Metallothionein Complex

Metallothionein is a low molecular weight protein found in the kidney and liver. It has been implicated in the metabolism of cadmium, zinc, copper, and other metals. After treatment with gold(I) or gold(III), metallothionein is known to contain a mixture of metals with bound gold, cadmium, and zinc, depending on experimental conditions.[18] It has been suggested that metallothionein may be the site of interaction with essential trace elements. The cadmium binding sites were first investigated by ^{113}Cd NMR studies,[39-41] and an EXAFS study of the zinc sites was reported.[42] Results from both types of studies indicated that Cd(II) and Zn(II) ions occupy four-coordinate sites. Subsequently, an X-ray single-crystal structure analysis was reported on rabbit liver metallothionein,[43] confirming four-coordinate, tetrahedral metal geometries for Cd and Zn. The gold binding site in metallothionein has recently been characterized by EXAFS spectroscopy and other complementary techniques.[44] When myochrisin is incubated with excess horse kidney metallothionein containing both zinc and cadmium, the zinc is preferentially replaced. Remarkably the EXAFS analysis shows that gold (which has replaced four-coordinate zinc) is coordinated by 2.4 sulfur atoms at a distance of 2.29 Å. Whether the gold is in two different sites, some of which are three-coordinate while others are two-coordinate, or the EXAFS coordination number is somewhat in error and all gold atoms are two-coordinate is difficult to ascertain. No matter the case, the propensity of gold for a low coordination number seems to have led to a reworking of the protein metal binding sites. The changes in protein structure are small enough that little difference is found in chromatographic or antigenic behavior.[44] To check this rather startling result that gold remains two-coordinate, EXAFS spectra for two AuS_4 complexes of known crystal structure were measured and fit, yielding coordination numbers of 3.9 and 4.1. This test of AuS_4 systems as well as the previous fits of AuS_2 compounds shows that coordination number can be adequately determined for AuS materials, thus strengthening the argument that gold modifies the metallothionein conformation sufficiently to create two-coordinate sites for itself. Since our report of two-coordinate gold binding in metallothionein there has been a report of a rat liver metallothionein containing copper. The EXAFS spectrum[45] of this protein has been interpreted to show three-coordinate metal geometry giving another indication that all metallothioneins need not contain four-coordinate metals.

E. Aurosomes, Algae

A consequence of chrysotherapy is the accumulation of gold deposits in kidney, liver, and other tissues. The location of the gold deposits appears to be specifically in lysosomes, hence the name "aurosomes". These were morphologically described by electron microscopy by Ghadially in 1979.[21] Typically, aurosomes are filamentous aggregates with diameters of a few microns. The chemical form of the gold in aurosomes remained unknown, prior to our studies.[27,28]

The samples used in this EXAFS and XANES study were kidney aurosomes derived from laboratory animals undergoing gold therapy. Samples of aurosomes derived from myochrisin, auranofin, and $[AuCl_4]^-$ were obtained. The XANES spectra of the aurosomes identified the oxidation state of the gold as 1+. The aurosomes originating from the gold pharmaceuticals myochrisin and auranofin had the same oxidation state as the drugs. An oxidation state of Au(I) in the aurosomes derived from gold tetrachloride demonstrated that in vivo reduction occurred. It is surprising that reduction and deposition of the gold happened so quickly. These aurosomes were extracted 18 h after a single injection of the gold(III) chloride salt. Thus, reduction of Au(III) to Au(I) and accumulation of gold in the kidney aurosomes occurred within that time period.

The auranofin XANES spectrum was used to determine whether the gold–phosphorus bond was present. If phosphorus ligation were intact, one would expect to see the edge-rise feature characteristic of a gold–phosphorus bond. In Figure 6, the edge spectrum of auranofin-derived aurosomes is compared with that of auranofin. It is clear that the phosphorus "signature" is absent. This finding, in conjunction with our study[37] of auranofin after gut absorption, implies that at some point after absorption through the intestinal wall the auranofin Au–P bond has been cleaved. Conceivably,

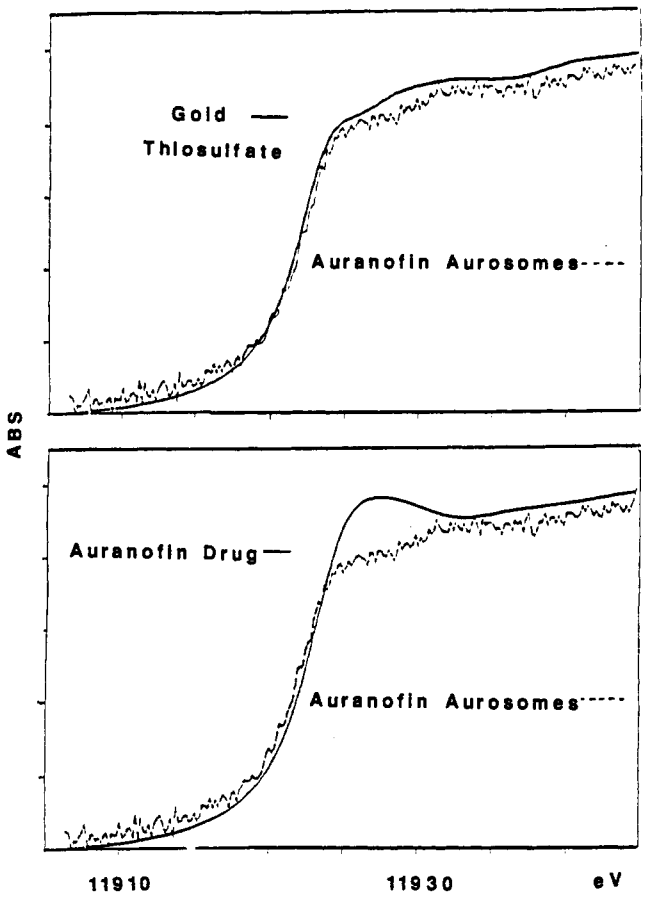

Figure 6. XANES spectra from aurosomes developed in response to auranofin dosage compared with those from the starting drug and bis(thiosulfato)gold(I) XANES. Cleavage of the Au–P bond occurred before aurosome formation.

the bond cleavage could occur within the aurosomes themselves. A study with dogs[46] has shown that triethylphosphine oxide is produced as a drug metabolite, proving Au–P cleavage in at least one instance.

Structural information about the gold in aurosomes[27] was obtained by EXAFS curve fitting. The gold in myochrisin-derived aurosomes was determined to be bound by 2.2 sulfur atoms at 2.30 Å. Since the gold coordination sphere appears identical with that of the drug, it is not possible to tell the extent of metabolism that myochrisin has undergone. The possibility that aurosomes may be a storehouse for the drug cannot be excluded in this case. However, myochrisin-induced and auranofin-induced aurosomes have indistinguishable spectra, suggesting similar material in the aurosomes. Since the auranofin-induced aurosome has no gold–phosphorus coordination, it must contain a gold metabolite. Therefore, we suspect that the myochrisin-induced aurosome may contain metabolized drug as well.

EXAFS analysis of the aurosomes originating from gold tetrachloride showed that the gold could be described equally well by two sulfur atoms bound at 2.30 Å or two chlorine atoms at 2.29 Å. The Au–S results are preferred, however, based on the chemical likelihood of an Au(I) two-coordinate sulfur structure. The existence of a stable $Au^{I}Cl_2$-type structure has not been shown. These results demonstrate that gold(III) tetrachloride is metabolized rapidly when injected into the body. The XANES spectrum reveals that Au(III) is reduced to Au(I). The EXAFS results show that the four chloride ions of the starting material have been displaced by two sulfur ligating atoms.

As another example of studies of gold in a biological milieu, we have recently used EXAFS and XANES to study the interaction of gold with biomass obtained from the algae *Chlorella vulgaris*.[47] The interest in this area is driven by the possiblity of recovery of gold from mine tailings in an economically viable, nonpolluting process. Our general findings are similar to those given above: gold(III) is reduced to gold(I) in the presence of algae, and that product will preferentially have gold(I) bound two-coordinate by sulfur. Gold(I) as the dicyano complex will undergo substitution to bind to sulfhydryl sites in the biomass.

The biological chemistry of the gold-based drugs is becoming clearer. The predominant gold oxidation state in the body is 1+. Sulfur coordination by thiolate sulfur is preferred, with bridging by thiolate favored over coordination by oxygen of a carboxylate, as in the drug sodium gold(I) thiomalate. The Au coordination number will be at least 2 with binding to nitrogen (or oxygen) donors if needed to achieve two-coordination. Reduction of gold(III) to gold(I) appears to occur quickly as does thiolate exchange.

F. XAS of Gold-Biological Samples, Summary

X-ray absorption spectroscopy has become a valuable tool in studies of rheumatoid arthritis treatment with gold-based pharmaceuticals. Samples taken, for example, from kidney tissues of rats may be directly examined and gold oxidation state, coordination number, type of ligating atom, and bond distance may be determined. Twenty milligrams of material is sufficient for the experiment. Currently, concentrations of millimolar or higher levels are required. Therapeutic levels in most tissues and fluids are $^1/_{10}$th to $^1/_{20}$th this amount, and an improvement in sensitivity will dramatically increase the number of samples that can be fruitfully studied.

Questions still remain concerning the extended structure in metallothionein containing gold and in kidney aurosomes. Whether the oligomers characteristic of the pure drugs have any existence in the body remains to be answered. The X-ray scattering experiments discussed in section V are starting to shed some light on these questions.

II. Technetium Radiopharmaceuticals

Since 1950, technetium radiopharmaceuticals have become the most important class of diagnostic imaging agents. One-third of all patients admitted for an overnight hospital stay are diagnosed by a Tc scan.[7,48-50] In outline, a radioactive material based on ^{99m}Tc is injected and collects at the organ of interest. Decay of the metastable ^{99m}Tc to its ground-state ^{99}Tc is accompanied by emission of a γ ray. A γ camera then produces an image as shown in Figure 7 wherein a bone-scanning agent has been used to image skeletal features. Notice, however, that the joints of the knees and ankles stand out as do the ends of the ribs, whereas the long bones of the legs are difficult to discern. For this imaging agent, the growing surfaces of the bones preferentially take up the ^{99m}Tc. This uptake pattern then makes such an agent useful in screening for the development of bone cancer or for following the mending

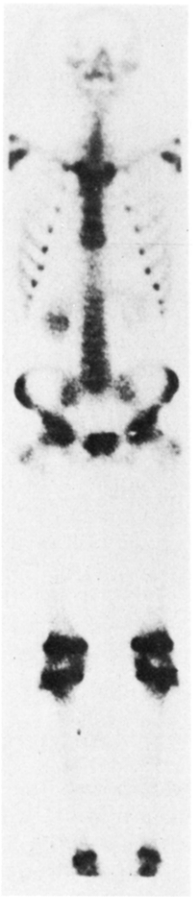

Figure 7. Technetium bone image with some "X-ray"-like features but showing sites of active uptake of the radiopharmaceutical.

process of broken bones. A variety of ^{99m}Tc agents[48–50] have been developed to image and lungs, liver, bones, or brain, for example. The general requirements for a good imaging agent are that it is readily available, forms high-contrast images with little or no toxicity or tissue damage, and clears rapidly from the body. The 6-h half-life of ^{99m}Tc is nearly ideal as it is long enough for some chemical syntheses but short enough that agents that clear only slowly contribute very little radiation after 1 or 2 days. For high-contrast images, a single pure compound with high-binding affinity for a particular organ is desirable. Since the preparations contain extremely small amounts of technetium in high dilution (10^{-6}–10^{-8} M), it has been difficult to characterize chemically some of the imaging agents in use. One strategy used by Deutsch and his group[51] at the University of Cincinnati has involved chromatographic separation of reaction products followed by tissue-distribution studies on the separated materials. Synthetic methods may then be optimized to produce materials of interest in high yield, and those agents may be more fully characterized by various techniques. The characterization technique we emphasize here is, of course, EXAFS spectroscopy.

In the previous studies on gold drugs considerable benefit accrued from the ability to obtain EXAFS from biological samples such as the auranofin metabolite that passed through the gut wall or aurosomes obtained from rat kidneys. For the technetium imaging agents, this approach has not been feasible due to the extremely low concentrations at which these radiopharmaceuticals are

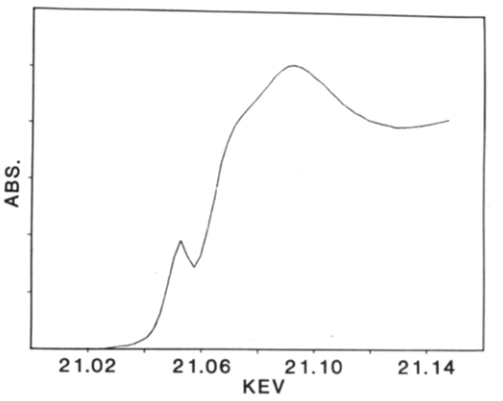

Figure 8. XANES of the TcO_4^- ion showing the "yl" oxygen feature on the low-energy side of the edge.

used. However, the applicability of EXAFS to noncrystalline materials has proven to be quite helpful. In one instance we have been able to derive detailed information from EXAFS that we could not obtain from a crystal structure, and in another we have been able to characterize the structures of solution species of bone imaging agents.

A. Features of Tc EXAFS and XANES

Tc spectra are measured for the K absorption edge at 21.047 keV, a similar energy to that used for the more standard studies of molybdenum complexes such as nitrogenase and its models. The experimental difficulties are similar to Mo studies, with the paucity of X-ray photons at these higher energies becoming a significant problem. The lack of resolution plus line width broadening at these energies seems to make XANES a less useful tool than with gold, although a Tc=O signal can be seen at 21.05 keV in the XANES of a NH_4TcO_4 sample as shown in Figure 8. The intensity of this feature appears to be a special case for the tetrahedral TcO_4^- anion, and it has not been possible to develop a general diagnostic for the "yl" oxygen in a Tc=O moiety. The "yl" oxygen XANES signature has been noted and used for other metals such as vanadium,[52] however.

A further experimental difficulty deserving comment for Tc complexes involves radioactivity. All isotopes of technetium are radioactive, and all are man-made. Since technetium as ^{99}Tc is a relatively abundant fission product of uranium, it is a reasonably cheap material, costing less than rhenium for instance.[7] The ground-state ^{99}Tc is radioactive, giving off a low-energy β particle with a half-life of 2.1×10^5 years. Thus, for EXAFS studies we use ^{99}Tc materials as opposed to the ^{99m}Tc materials which are the actual imaging agents. Due to the inherent radiation hazards and problems associated with spills of a material with a 2.1×10^5 year half-life, samples normally are prepared in sealed cells in Cincinnati and not opened at SSRL. In the relatively rare cases where we have used liquid samples containing technetium, glovebag containment of liquids until they have been sealed into cells has proven satisfactory.

B. Technetium Halide and Oxyhalide Complexes

The chemical form of ^{99m}Tc available for synthesis of imaging agents is TcO_4^-, which may be eluted with saline solution from alumina loaded with $^{99}MoO_4^{2-}$. The

TABLE I. Results of EXAFS Analysis on TcX_6^{2-}, $TcOX_4^-$, and $TcOX_5^{2-}$ Complexes

Tc complex		EXAFS analysis		crystallographic analysis	
		R,[a] Å	N[b]	R, Å	N
$TcCl_6^{2-}$	Tc–Cl	2.37	6.1	2.35	6
$TcBr_6^{2-}$	Tc–Br	2.52	6.8	2.52	6
TcI_6^{2-}	Tc–I	2.72	6.0		
$TcOCl_4^-$	Tc–O	1.65	1.3	1.61	1
	Tc–Cl	2.30	3.0	2.31	4
$TcOCl_5^{2-}$	Tc–O	1.65	1.2		
	$Tc–Cl_{cis}$	2.36	3.6		
	$Tc–Cl_{trans}$	2.50	0.8		
$TcOBr_4^-$	Tc–O	1.66	1.4		
	Tc–Br	2.48	5.4		
$TcOBr_5^{2-}$	Tc–O	1.66	1.0		
	$Tc–Br_{cis}$	2.54	5.4		
	$Tc–Br_{trans}$	2.74	1.6		

[a] R is bond distance. [b] Number of atoms of this type bound to Tc.

molybdate-99 decays to form pertechnetate-99m. This monoanionic species is eluted under conditions where the parent dinegative molybdate remains tightly bound. To form imaging complexes, the TcO_4^- is generally reduced and also substituted with ligands thought to provide specific transport or binding properties such as various diphosphonates used in bone-imaging agents or arsines, phosphines, and isocyanides used to generate lipophilic Tc complexes for possible heart-imaging agents.

One group of reducing agents of interest are the hydrohalic acids, which have been used to produce a variety of synthetic intermediates, TcX_6^{2-}, $TcOX_4^-$, and $TcOX_5^{2-}$, which may then be used to form further Tc(V) and Tc(IV) complexes via a substitution route.[7,48] Many of the synthetically useful technetium complexes have been characterized fully by X-ray crystal structure determinations;[7,53] however, for this particular series we have been unable to crystallize any form of TcI_6^-, $TcOBr_4^-$, $TcOCl_5^{2-}$, or $TcOBr_5^{2-}$. Thus, in this series, EXAFS provides the base of structural information. Results of the various fits are given in Table I. For the octahedral hexahalo complexes fits were derived from theoretical amplitudes and phases (TAP) as suggested by Teo and Lee.[54] For the chloride and bromide cases the agreement with the known crystal structure is quite good. The increase of 0.20 Å on going from $TcBr_6^{2-}$ to TcI_6^{2-} is in good agreement with the increase of 0.21 Å expected from Pauling's crystal radii[55] for Br^- and I^-. Although the TAP approach works well for those cases where the absorbing atom has one type neighbor only and all neighbors are at the same distance, it becomes cumbersome to unworkable with different atom types and/or similar atoms at different distances. A more recent version of the theoretical approach using fine adjustment based on models (FABM)[56] is considerably more promising, however. At the time of our studies, we used the empirical approach[14] for the other complexes listed in Table I, basing the transferable parameters on the model compounds $KTcO_4$, $[(n\text{-}Bu)_4N]_2[TcCl_6]$, and $[(n\text{-}Bu)_4N]_2[TcBr_6]$. Although only one direct comparison with a crystal structure is possible, several other indirect evaluations encourage us to believe that the EXAFS results are quite reliable.[57] In $TcOX_5^{2-}$ the one X group trans to the "yl" oxygen is expected[53,58] to be significantly further from Tc than the four cis groups due to the structural trans effect (STE). The STE for Cl^- is 0.14 Å and for Br^- is 0.20 Å. Second, the cis groups are expected to be more distant from Tc in the six-coordinate structure than in the five-coordinate $TcOX_4^-$.[59] Thus, $Tc–Cl_{cis}$ in $TcOCl_5^-$ is 2.36 Å, essentially the same as the value of 2.35 Å for $TcCl_6^{2-}$. For $Tc–Br_{cis}$ in $TcOBr_5^{2-}$ the value of 2.54 Å compares to 2.52 Å for $TcBr_6^{2-}$. Finally, the value of the metal–oxygen distance, 1.65 Å, is invariant to change in X group or technetium coordination number as would be expected from a comparison with the known molybdenum analogues[60-62] and agrees with the value of 1.66 Å determined for the Tc=O distance in $[Tc(DMPE)_2(O)(OH)]^{2+}$ as described below.

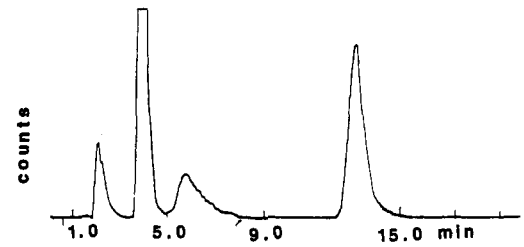

Figure 9. High-performance liquid chromatogram of reaction products from ammonium pertechnetate and 1,2-bis(dimethylphosphino)ethane (DMPE) in normal saline. The peaks in order of elution time represent TcO_4^-, $[Tc(DMPE)_2O_2]^+$, $[Tc(DMPE)_2Cl_2]^+$, and $[Tc(DMPE)_3]^+$.

C. Technetium Complexes with Phosphine-Containing Ligands

One organ for which there currently is no clinically available Tc imaging agent is the heart. Davison and co-workers[63,64] developed a series of low-valent lipophilic Tc(I) cationic species based on isocyanide ligands, $[Tc(CNR)_6]^+$, where the exact properties of the proposed imaging agent may be modified by changing the R group of the isocyanide. Recently some of these have undergone clinical testing.[65] Deutsch and his group have also developed a series of low-valent Tc complexes using neutral, bidentate ligands based on phosphines such as 1,2-bis(dimethylphosphino)ethane (DMPE) and 1,2-bis(diphenylphosphino)ethane (DPPE). Several interesting problems arose in the course of characterizing these complexes where EXAFS was able to provide information unavailable by other means.

The preparation of the phosphine-based complexes utilizes TcO_4^- with excess ligand. The phosphine both serves as a reducing agent and binds the technetium. Under nonoptimized conditions a variety of products in various oxidation states are formed as shown in the chromatogram (Figure 9). The component with the longest retention time showed some promise as a heart imaging agent, and further characterization was desired. The material could be crystallized, and analysis indicated a likely cationic complex, $Tc(DMPE)_3^+$, although other formulations were possible. Crystals of the material as the F^-, ClO_4^-, or PF_6^- salts were so badly disordered that the structure could not be unequivocally determined. EXAFS data were obtained for $[Tc(DMPE)_3]F$ and the Fourier transform gave rise to a single, somewhat asymmetric, peak, suggesting that only one type of atom (phosphorus) was necessary to model the coordination sphere. A TAP fit was utilized, which gave six neighbors at 2.40 Å in agreement with expec-

TABLE II. Results of EXAFS Analysis on Tc-P Complexes

complex		EXAFS, analysis R, Å	N	crystallographic analysis R, Å	N
$[Tc(DMPE)_3]F$	Tc-P	2.40	6.0		
$[Tc(DMPE)_2(O)(OH)](F_3CSO_3)_2$	Tc-P	2.46	4.1	2.48 av	4
	Tc-O	1.66	0.9	1.80	2
	Tc-O	1.96	0.7		
$[Tc(DMPE)_2Cl_2]Cl$	Tc-P	2.45	4.7	2.44 av	4
	Tc-Cl	2.31	1.8	2.32 av	2
$[Tc(DMPE)_2Br_2]Br$	Tc-P	2.44	4.0		
	Tc-Br	2.51	1.6		
$[Tc(DPPE)_2Cl_2]Cl$	Tc-P	2.50	4.0	2.50 av	4
	Tc-Cl	2.30	2.4	2.32	2
$[Tc(DPPE)_2Br_2]Br$	Tc-P	2.47	3.8	2.50 av	4
	Tc-Br	2.44	2.9	2.44	2

tation. The TAP approach was essential since there were no single-shell Tc–P model compounds available. In order to test the validity of the TAP results, we adopted a hybrid TAP/empirical approach.[66] The data for $[Tc(DMPE)_3]F$ were fit with the standard six-parameter, empirical approach of Hodgson and co-workers.[14] These could then be treated as transferable parameters from a known model compound with the distance of 2.40 Å and coordination number 6 known from the TAP calculation. The transferable parameters were then used to fit a variety of multishell complexes as indicated in Table II. The quality of the fits was good and the excellent agreement with single-crystal, X-ray diffraction results satisfying. Clearly the transferable Tc–P parameters provide good bond lengths and coordination numbers in all cases, and thus we had a high level of confidence in the $[Tc(DMPE)_3]^+$ TAP results, which provide the basis for the transferable parameters.[66] Interestingly, a single crystal of the $[B(C_6H_5)_4]^-$ salt was subsequently produced by Du Pont workers and its structure determined to give a Tc–P bond[67] average length of 2.39 Å in remarkable correspondence to our EXAFS value.

One case in Table II deserves special mention. It is an interesting situation in which EXAFS is able to provide more structural detail than single-crystal, X-ray diffraction. The crystal structure of $[Tc(DMPE)_2(O)(OH)](F_3CSO_3)_2$ has been solved by diffraction techniques in our laboratory.[66] The technetium atom is at an inversion center in the space group $P2_1/c$, and so the oxo and hydroxo moieties must be disordered. As a result, only an average Tc–O distance of 1.80 Å is obtained in a structure that refines well to a residual of 5.0%. EXAFS, on the other hand, is not troubled by the disorder, and a three-shell fit refines well as shown in Figure 10 with a Tc=O of 1.66 Å and a Tc–OH of 1.96 Å. Note that the average of these values, 1.81 Å, agrees with the disordered crystal structure value and the Tc=O value agrees well with that distance determined in other single-crystal diffraction experiments. One up for EXAFS!

D. Unsolved Problems with Tc-Based Imaging Agents

The most basic difficulty arises because the imaging agents are used at extremely low concentrations (10^{-6}–10^{-8} M) in solutions. EXAFS deals well with solution species but currently can be used routinely only for concentrations of 10^{-3} M and greater. No developments now foreseen are likely to increase EXAFS sensitivity by 3–5 orders of magnitude, and it appears that a direct experiment on an imaging agent in the biological milieu will not be possible. The next best approach seems to require a technique with high sensitivity and specificity and also a wide range of sensitivity to bridge the gap between solutions suitable for EXAFS and those used in actual imaging. High-performance liquid chromatography (HPLC) with radiometric, electrochemical, and/or inductively coupled plasma mass spectral detection shows promise. The HPLC provides the high level of specificity to separate individual components, and these detection methods have the sensitivity to operate at 10^{-8} M. The detection methods also have the dynamic range necessary to operate in relatively concentrated solutions (10^{-2} M) where EXAFS structure determination is practical. Thus, it is possible to determine the structure of a particular agent in solution and then show that this same material persists at the low concentration levels of the actual imaging process. It seems likely as access to EXAFS facilities becomes more widespread that this approach will be adopted. The advantages of direct structural information from solution species are considerable after all. We have recently used this approach to study the technetium diphosphonate bone-imaging agents with considerable success.[68,69]

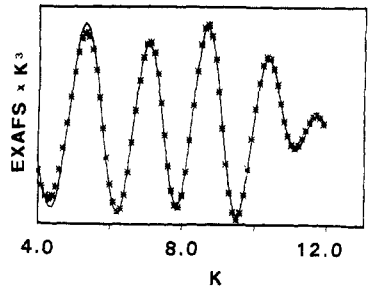

Figure 10. EXAFS curve fit for the structure of $[Tc(DMPE)_2(O)(OH)](F_3CSO_3)_2$. Asterisks represent filtered data points and the solid line the calculated values from the empirical fit.

A particularly vexing problem with technetium imaging agents involves the ubiquitously applied stannous ion reducing agents; that is, TcO_4^- is reduced with stannous ion in the presence of the ligand of choice to form the imaging agent. Both Sn-labeling experiments[70] and a binuclear crystal structure incorporating tin, technetium, and dimethylglyoxime[71] show that tin frequently "follows" the technetium. Clearly EXAFS is possible for tin (although the K absorption edge is at 29.195 keV and the L_I edge is at 4.465 keV, neither particularly convenient), and thus it is possible to determine whether tin is present in any isolated technetium imaging agent analogue. However, it is not currently possible to determine the structural relationship between tin and technetium unless they are within approximately 4 Å or less. This failure of EXAFS to reveal second neighbors was particularly frustrating in early studies of molybdenum enzymes where evidence of an Fe–Mo interaction was suspected.[72] Cramer and Scott have measured EXAFS at liquid helium temperatures in an effort to gain information about more distant interactions. The hope is that by minimizing the thermal disorder in a structure the damping out of longer range information will be lessened. This ap-

proach is meeting with some success. Recently the Mo–Fe interaction in nitrogenase was clearly observed in data collected at 4 K.[73] Thus, under similar measuring conditions, EXAFS might shed some light on the tin–technetium association. A similar problem that needs longer range information than the first coordination sphere involves the technetium diphosphonate complexes where polymeric species are thought to form but little definite information on structure is available.[7,48,74] These complexes are thought to act as bone-imaging agents due to bridging between technetium and the exposed calcium of bones by the diphosphonate ligands. Some EXAFS information from data at liquid helium temperature which illuminated these structures would be extremely helpful. A different approach, that of using wide-angle X-ray scattering (WAXS) and differential anomalous scattering (DAS) to obtain longer range information, is suggested in the final section of this paper.

We are now investigating a third approach, that of differential EXAFS[75] for this problem. In essence, if the EXAFS spectra of two complexes with identical first coordination spheres are subtracted from each other and the difference data processed normally, then the result should have the short-range information "subtracted out" and the remainder should describe the differences in the longer distances. Our studies of $[Co(en)_3]^{3+}$ and the complex with the encapsulating sepulcrate ligand,[76] $[(Co(sep)]^{3+}$, have shown clearly that the method works. Studies of calcium and strontium precipitates of technetium diphosphonate complexes not only indicate the Tc–O bonds in the first coordination sphere and the presence of phosphorus at a further remove but also substantiate the polymeric nature of the complexes by giving a clear indication of a third-shell technetium–technetium interaction.[75]

While this difference methodology may help in the visualization of weak features in the Fourier transform, it is important to realize that errors in measurement for either partner become correspondingly more important and also that small changes in structure between two "identical" sites will be emphasized by this process. Thus, the interpretation may not be as easy as hoped.

III. Platinum Anticancer Drugs

In 1969, Rosenberg[77] reported that platinum–ammine complexes with cis configuration were chemotherapeutic agents. Currently, *cis*-diamminedichloroplatinum(II) (*cis*-DDP) is widely used for treatment of testicular, ovarian, and bladder cancers[78] and is considered to be curative.[79] In the relatively short period of time since 1969, enormous research effort has gone into understanding the reactions of *cis*-DDP with its presumed target, DNA. *cis*-DDP is thought to inhibit replication of cellular DNA through intrastrand cross-linking of DNA base pairs.[80] Interestingly, the drug action is stereospecific; the trans isomer does not exhibit antitumor activity, perhaps because its damage is more rapidly repaired.[81] At the present time, Lippard[80] and co-workers seem to have answered most of the structural questions concerning *cis*-DDP binding to DNA, namely that the *cis*-$(NH_3)_2Pt^{2+}$ residue binds covalently to N(7) of each of two adjacent guanines and thereby disrupts base stacking in the DNA. However, prior to 1985 a number of investigators used EXAFS techniques to provide the initial understanding of the *cis*-DDP–DNA binding problem.

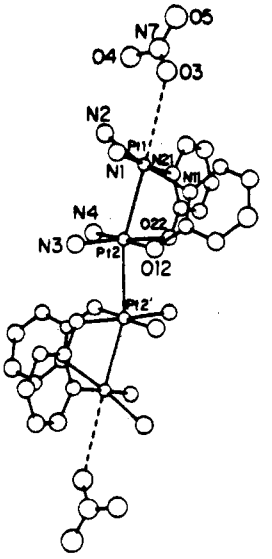

Figure 11. Structure of the α-pyridone "platinum blue" tetramer. Reprinted with permission from: Barton, J. K.; Rabinowitz, H. N.; Szalda, D. J.; Lippard, S. J. *J. Am. Chem. Soc.* **1977**, *99*, 2827. Copyright 1977 American Chemical Society.

A. Platinum "Blues" and Hydroxo-Bridged Species

The reactions of *cis*-DDP in water are many, as are its reactions with DNA. The reaction of *cis*-DDP with the nucleic acid building blocks uracil and thymine yields blue colored complexes classed as "platinum blues". These species exhibit antitumor activity with less toxic side effects[82] than *cis*-DDP. Although somewhat rare, blue platinum complexes have been known for a long time. Little was known about them because they are polymeric with variable chain lengths and difficult to crystallize. In 1977, Lippard and co-workers,[83] using α-pyridone with its ketonic oxygen adjacent to the amine function in the ring, were able to mimic the nucleic acid–platinum interaction and form a blue crystalline solid. The crystal structure, shown in Figure 11, revealed a tetrameric unit formed by the centrosymmetric junction of two α-pyridone-bridged dimers. The dimeric units are of the "head-to-head" kind, where one platinum atom binds two cis ammonia groups and the oxygen atoms of two α-pyridones. The other platinum atom in the dimeric unit then binds two cis ammonia groups and the nitrogen atoms of the two α-pyridone bridges to yield a platinum–platinum distance in the dimer of 2.8 Å. Given the head-to-head dimers, two PtO_2N_2 units can join by a 2.9 Å Pt–Pt bond to form the tetramer. There are five nitrate counterions, which leads to the formal oxidation states of three Pt(II) and one Pt(III). A low-energy transition involving the metal–metal bonding electrons leads to the blue color. This explanation, that the blue color involved a metal–metal bond, suggested that such bonding might be an important aspect of *cis*-DDP binding to DNA. The recently determined structure[80] shows no evidence of metal dimers, but in 1977 an intense search took place.

Studies of the hydrolysis reactions of *cis*-DDP have shown a variety of products resulting from the initial replacement of chloride by water. Interestingly the

further reactions lead to the formation of hydroxo-bridged dimers, trimers, and tetramers. Crystal structures have been determined for several platinum, hydroxo-bridged dimer and trimer complexes, $[(NH_3)_2Pt(OH)]_2^{2+}$[84,85] and $[(NH_3)_2Pt(OH)]_3^{3+}$.[86,87] The platinum–platinum separation in the dimeric structures is about 2.95 Å. Here again, although from a different point of view, there was a suspicion that relatively short (2.9 Å) platinum–platinum distances might be found when *cis*-DDP binds to DNA. It should be noted, however, that the hydrolysis reactions are not likely to occur until the drug passes across the cell membrane and encounters a reduced chloride ion concentration.[82] In fact, it is generally agreed that the dichloro form of the drug itself is not the active agent but rather that the hydrolysis products are active.

Both of the observations above suggested that EXAFS could be a useful probe for dimer formation in *cis*-DDP binding to purines and pyrimidines. As mentioned previously, anticancer activity has been reported for platinum–pyrimidine blue complexes. Teo and co-workers[88] measured the Pt L_I EXAFS of products derived from the reaction of uridine with *cis*-Pt-$(CPA)_2Cl_2$ (CPA = cyclopropylamine) to give a purple complex and *cis*-$[Pt(NH_3)_2(H_2O)_2]^{2+}$ to yield a blue complex. The Fourier transforms of the EXAFS for these two compounds are shown in Figure 12. Atom identifications were made by comparison of the Fourier transforms to those of the structurally characterized complexes $Pt(en)_2$ and $Pt(en)(Guo)_2$ (en = ethylenediamine, Guo = guanosine). Neither of the known structures have a Pt–Pt bond. The major peaks in the spectra of the blue and purple complexes were assigned to light scatterers, either N or O, or conceivably C, emphasizing the point that EXAFS analysis fails to decipher the identity of these light atom scatterers. This is a severe handicap here because identifying the platinum binding site on pyrimidines or purines requires the ability to distinguish carbon, nitrogen, and oxygen.

The existence of a Pt–Pt interaction in the platinum–uridine complexes was determined from the EXAFS. The third peak (labeled B, Figure 12) in the Fourier transforms of platinum–uridine blue and platinum–uridine purple was identified as a platinum back-scatterer by observing the increasing k weighting of the EXAFS data with respect to a reference peak. Since heavy scatterers have EXAFS envelopes with maxima at higher k values, the ratio of peak amplitudes should increase because of increasing weighting on the higher k range (assuming that the reference peak is from a scattering atom of low atomic number).

The intermediate peak in the Fourier transforms of these species could not be readily assigned due to overlap from the major peak. Curve-fitting analysis was performed on filtered, back-transformed data of all three peaks. A Pt–N distance of about 2.0 Å was obtained as well as a Pt–C (or oxygen) distance at about 2.4–2.6 Å and a Pt–Pt distance of about 2.9 Å in both complexes.

This work substantiated the presence of the Pt–Pt bond in platinum–pyrimidine complexes. The binding site of the platinum on uridine could not be determined from the EXAFS. Contributions from outer shells of atoms originating with the uridine ring are negligible.

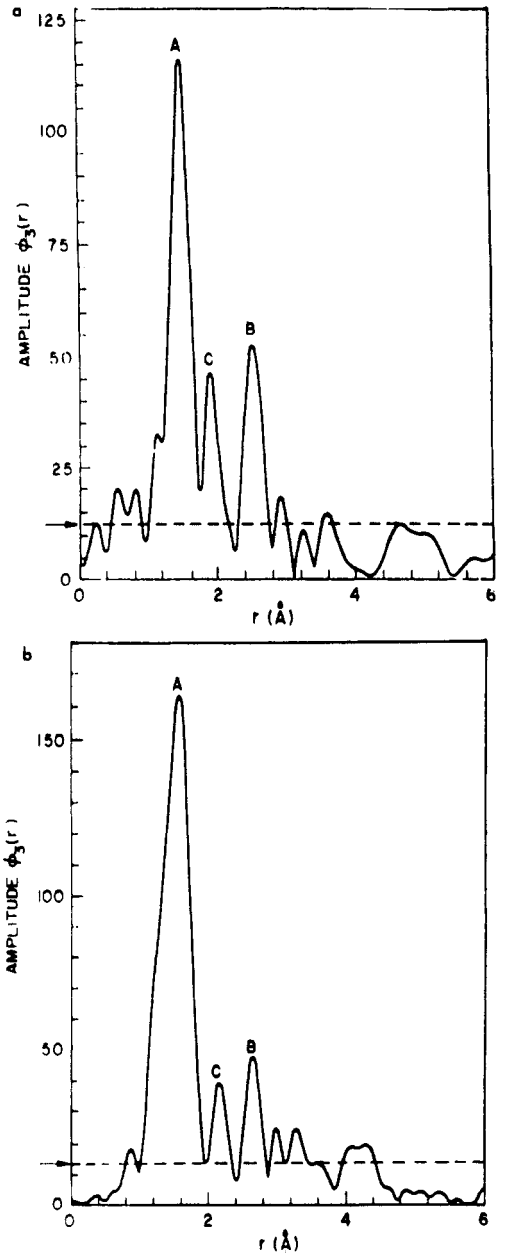

Figure 12. Fourier transforms of the EXAFS from (a) platinum uridine purple and (b) platinum uridine blue as published by Teo and co-workers. The peaks labeled B represent a Pt–Pt interaction. Reprinted with permission from: Teo, B. K.; Kijima, K.; Bau, R. *J. Am. Chem. Soc.* **1978**, *100*, 621. Copyright 1978 American Chemical Society.

Second- and third-shell scatterer identification would presumably be valuable for determining the binding site on uridine. However, Teo suggested plausible structures based on the determined distances and other structures of analogous systems. One such structure involves an oligomeric chain of platinum atoms coordinated to N3 and O4 (or N3 and O2) of stacked uridinates in a square-planar configuration. This type of structure would have a PtNCO four-membered ring with a Pt–C distance comparable to 2.5 Å, in agreement with the intermediate peak in the Fourier transform. Another possible structure would be analogous to the known structure *cis*-$Pt(NH_3)_2$(α-pyridone).

B. *cis*-DDP–DNA Complexes

The observation of the Pt–Pt bond in the "platinum blue" compounds prompted researchers to question

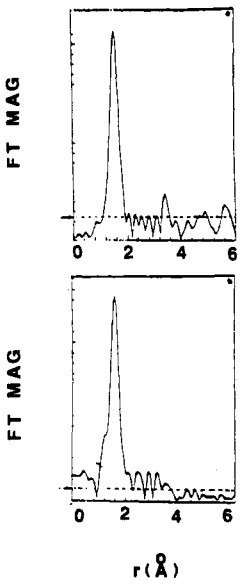

Figure 13. Fourier transforms of EXAFS data of (a) *cis*-DDP bound to DNA and (b) *trans*-DDP bound to DNA as published by Teo and co-workers. There is no evidence of a short Pt–Pt interaction. Reprinted with permission from: Teo, B. K.; Eisenberger, P.; Reed, J.; Barton, J. K.; Lippard, S. J. *J. Am. Chem. Soc.* 1978, *100*, 3225. Copyright 1978 American Chemical Society.

whether that bond is found in the reaction products of *cis*-DDP with DNA. EXAFS investigations were carried out in separate studies by Teo et al.[89] and Hitchcock et al.[90] Teo measured the EXAFS of the product generated by reacting each isomer, *cis*- and *trans*-Pt$(NH_3)_2Cl_2$, with calf thymus DNA. The Fourier transforms of the EXAFS data are shown in Figure 13. The authors analyzed the Fourier transforms by comparison with that of [Pt(en)(Guo)$_2$], which has no Pt–Pt bond, and the platinum–uridine blues, which as mentioned, contain Pt–Pt bonds at about 2.9 Å. The Fourier transforms of both *cis*- and *trans*-DDP with DNA clearly lack a component that might reflect a Pt–Pt bond. Curve fitting by theoretical methods revealed that 4.3 nitrogen (or oxygen) atoms were bound to platinum at 2.025 Å in the *cis*-DDP–DNA adduct and 3.6 nitrogen (or oxygen) atoms bound to platinum at 2.033 Å in the trans analogue. Conceivably a high degree of thermal disorder could wash out the Pt–Pt signal in the EXAFS. However, the *cis*-DDP–DNA sample measured at liquid nitrogen temperatures gave data essentially identical with the corresponding room-temperature data.

Since the Pt L_I absorption spectrum occurs in the energy range around 14 keV, resolution of the data in the XANES region is sufficiently sharp to obtain information from the edge region of the spectrum. The L_I edges of the *cis*- and *trans*-DDP–DNA complexes were very similar to other known platinum(II) complexes, suggesting a Pt(II) square-planar configuration. A coordination number of 4 would be expected for a Pt(II) square-planar complex, which is in accord with the EXAFS determination of about four nitrogen atoms in the platinum coordination sphere.

The absence of the chloro ligands after binding to DNA was also demonstrated indirectly. Chlorine scatterers are distinct from nitrogen scatterers, and an interference pattern in the EXAFS would be expected if chloride ions were bound to platinum. The EXAFS spectrum consisted of a single sine wave component.

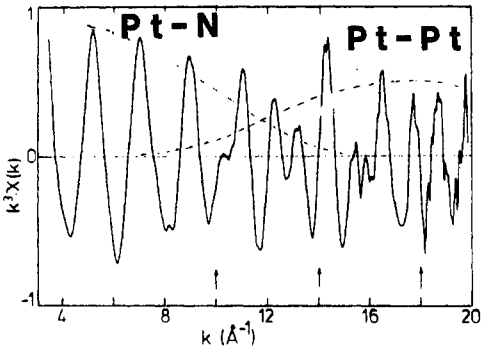

Figure 14. EXAFS spectrum, weighted by k^3, for the dimer $[(NH_3)_2Pt(OH)_2Pt(NH_3)_2](NO_3)_2$ showing the Pt–Pt contribution to the EXAFS at high k values. Reprinted with permission from: Hitchcock, A. P.; Lock, C. J. L.; Pratt, W. M. C.; Lippert, B. In *Platinum, Gold, and Other Metal Chemotherapeutic Agents*; Lippard, S. J., Ed.; ACS Symposium Series 209; American Chemical Society: Washington, DC, 1983; p 217. Copyright 1983 American Chemical Society.

No appreciable difference in the structures of the *cis*- and *trans*-DDP–DNA adducts was observed in the EXAFS. Stereochemical details of the platinum coordination sphere cannot be obtained from the EXAFS.

A controversy arose when Hitchcock examined the EXAFS of calf thymus DNA reacted with one of the *cis*-DDP aquation products, namely *cis*-$[(NH_3)_2Pt(OH)_2Pt(NH_3)_2]^{2+}$. The hydroxo dimer has been structurally characterized and its EXAFS measured. Its EXAFS spectrum (Figure 14) clearly shows evidence of the Pt–Pt bond, which is known to be at 2.95 Å. The beat pattern seen in the EXAFS multiplied by k^3 is indicative of multiple atom types and/or different distances to neighbors surrounding the absorber. The increasing amplitude in the k range from 14 to 20 Å^{-1} signals that one of the neighbors must be a heavy atom such as another platinum. Since the hydroxo dimer is generated from *cis*-DDP in water, it could conceivably be involved in the antitumor activity of *cis*-DDP. Although the platinum concentration inside a cell is expected to be low, Hitchcock[90] quotes a calculation[91] stating that the concentration of dimer $[(NH_3)_2Pt(OH)_2Pt(NH_3)_2]^{2+}$ will be at least 10^{-12} M. Lippard,[82] on the other hand, dismisses the dimer as unlikely to be a major intracellular component. Hitchcock and co-workers[92] originally saw evidence for a platinum–platinum bond in a sample of DNA incubated with the hydroxo dimer. They used variable k weighting in their Fourier transforms to improve visualization of the Pt–Pt peak. Figure 14 has dashed lines giving the envelope shapes for both Pt–N and Pt–Pt back-scattering. The dominance of the metal–metal interaction at high k is complete, and clearly Fourier transforms weighted heavily in k (k^4 or k^5) will emphasize the Pt–Pt peak.

The controversy subsided when followup studies of binding between the hydroxo dimer and DNA[93] by Hitchcock, Martins, and Lock gave no indication of a platinum–platinum interaction in the DNA-bound material. In a recent and very thorough study Hitchcock, Lock, and Lippert have documented[94] the types of dimers for which the platinum–platinum interaction may be observed. It is clear that if the two-hydroxyl, two-platinum core were to remain intact, the EXAFS would show the metal–metal interaction. It appears that the previous sample was not thoroughly washed free of the unbound dimeric starting complex. This

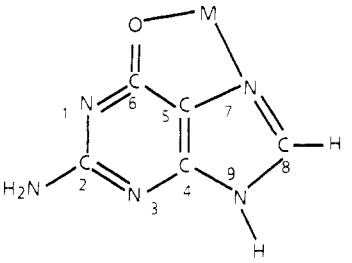

Figure 15. Guanine with a metal atom, M, bound to N7 and O6.

problem points out one of the inherent limitations in EXAFS studies. Although the EXAFS data are element specific (giving only neighbors to platinum in this case), they do average information over all absorber sites in the sample. There is no warning that two chemically distinct types of absorber are present such as platinum bound to DNA in some monomeric fashions and also residual starting platinum dimer.

C. *cis*-DDP–Guanine Binding

On the basis of a variety of studies by 1980, the guanine base was considered the most likely binding site for platinum.[95] One binding model involved the aquated $(NH_3)_2Pt(OH_2)^{2+}$ residue binding at N7 of guanine with added stabilization through an additional hydrogen bond between the coordinated water molecule and the exocyclic oxygen of the guanine ring. If platinum binds to N7 of guanine, there is also a possibility it will bind to O6 to form a five-membered chelate ring as indicated in Figure 15. Bruck, Bau, Teo,[96] and co-workers studied this question. No crystal structure determinations exist definitively demonstrating this mode of binding. However, a sulfur analogue of guanine, 6-mercaptoguanine, has been shown to form such chelates with several different metals, in particular Pd(II).[97,98] Structure determinations based on EXAFS were completed for 6-mercaptoguanine– and 6-mercaptoguanosine–platinum complexes as well as the analogous palladium complexes. *cis*-$Pt(NH_3)_2Cl_2$, Pd-(2-amino-6-mercaptopurineriboside)$_2$, and $Pd(Guo)_2Cl_2$ were used as model compounds. Data were measured in the transmission mode and collected to approximately 900 eV beyond the absorption edge. For the curve-fitting procedures, theoretical amplitude and phase functions were used. The Fourier-transformed data of *cis*-$Pt(NH_3)_2Cl_2$ and Pt(2-amino-6-mercaptoriboside)$_2$ are shown in Figure 16. The two peaks in the Fourier transform require the presence of two shells of scattering atoms. The calculated Pt–N bond distances are in the range 2.00–2.08 Å. The range of values for the Pt–S and Pt–Cl distances is 2.31–2.33 Å. Coordination numbers were determined to be about two nitrogen atoms and two chlorine or sulfur atoms. From the Fourier transform spectra, one can observe that the chlorine peak of the *cis*-DDP complex occurs at the same position as the sulfur peak of the Pt(2-amino-6-mercaptoriboside)$_2$ complex. Sulfur and chlorine back-scattering contributions to the EXAFS are similar, and their atom identities cannot be determined from the EXAFS. In this work, however, that ambiguity is not a problem because it is known that in the aqueous reactions of *cis*-DDP the chloride ions are displaced. Thus, the second Fourier transform peak in the Pt(2-amino-6-mercaptoriboside)$_2$ data is definitely due to

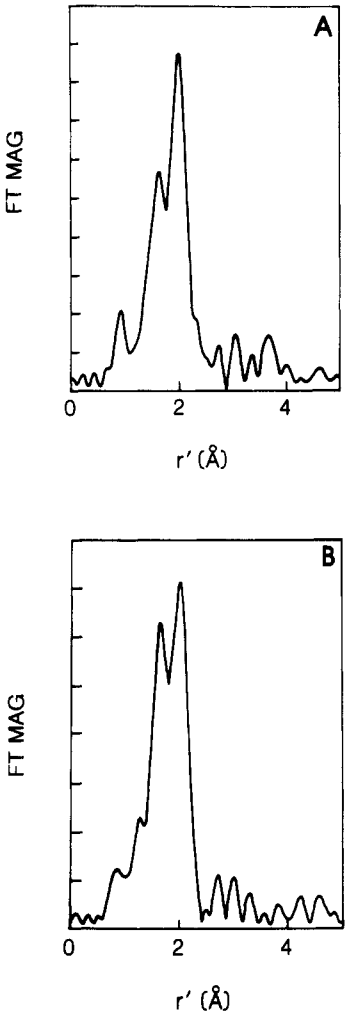

Figure 16. Comparison of the Fourier transforms of (A) *cis*-DDP and (B) Pt(2-amino-6-mercaptoriboside)$_2$. The highest peak in A represents Pt–Cl back-scattering, which is replaced by Pt–S back-scattering in B. Reprinted with permission from: Bruck, M. A.; Korte, H.-J.; Bau, R.; Hadjiliadis, N.; Teo, B. K. In *Platinum, Gold, and Other Metal Chemotherapeutic Agents*; Lippard, S. J., Ed.; ACS Symposium Series 209; American Chemical Society: Washington, DC, 1983; p 251. Copyright 1983 American Chemical Society.

sulfur scattering and not chlorine.

The authors note that the EXAFS structure analysis does not resolve the geometrical structure, whether the cis or trans configuration of the two mercaptoriboside ligands about platinum occurs. Furthermore, the authors point out that the existence of the N7–S6 chelate to platinum does not infer that the N7–O6 guanine–platinum complex will be formed.

D. Other Experiments

With the binding mode of platinum to guanine yet to be resolved, the Ph.D. studies of M. Bruck[99] included an attempt to determine whether the chelate-binding model was correct. This involved checking whether the Pt–C back-scatterer by the carbon atoms C5 and C6 of the purported chelate ring could be identified. No evidence for the chelate model was found. Bau[100] proposed a further experiment using 8-bromoguanine, which it was hoped would allow a clear distinction between chelated and nonchelated models based on the Pt–Br distance. As has been mentioned previously, second coordination sphere distances are difficult to

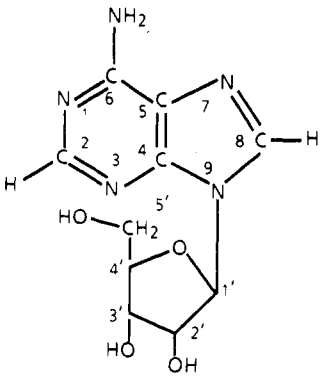

Figure 17. Structural formula of adenosine.

characterize unambiguously. In this case, interestingly, it should be possible to use the bromine EXAFS (Br K edge, 13.47 keV) to confirm any metal-based EXAFS conclusions; however, the experiment has not been carried out. The use of a "noninvolved" heavy-atom tag to extract stereochemical or conformational information from EXAFS is appealing but "noninvolvement" is difficult to guarantee as shown in the next section.

IV. Other Metals, Other Studies

A. Metal Anticancer Agents

The phenomenal success of *cis*-diamminedichloroplatinum(II) as a therapeutic agent for selected cancers[79] has led to investigations of other transition-metal ions as possible anticancer agents. The examination of palladium analogues to the antineoplastic platinum complexes by means of EXAFS spectroscopy[96] has already been mentioned in section IIIC. Other metal-based compounds showing antitumor activity include those based on ruthenium,[101], rhodium,[102] amine–chloride complexes, metallocene–dichloride complexes of the early transition metals such as Ti, V, Zr, Hf, Ta, Mo, and W,[103] a series of rhodium carboxylates,[104] and gold complexes such as auranofin[105] and its analogues.[1,106] EXAFS experiments have been performed on nucleoside adducts of the rhodium carboxylate complexes to probe the binding mode for the nucleoside. The experimenters[104] conclude that the spectra are best in agreement with N7 binding in adenosine (Figure 17) and its derivatives except in the case of 8-bromoadenosine. In that case, both Rh and Br EXAFS were examined and no evidence of the Rh–Br vector was detectable in either spectrum. The conclusion drawn was that the binding site had shifted to N1, yielding a Rh–Br distance too long for detection by EXAFS. The inference based on failure to observe the Rh–Br interaction seems dangerous based on our inability to observe Au–Au interactions with distances as small as 3.0 Å,[28] including cases with relatively rigid ring structures and gold–gold bonds. However, failure to bind the 8-bromoadenosine at N7 certainly seems reasonable, based on the steric constraint added by the bulky bromine. Use of a high atomic number tag such as Br to determine the binding site would be better demonstrated if a system could be found giving positive evidence of the proximity of the tag to the metal atom.

Clearly the binding of the other metal-based antitumor agents with nucleosides can be examined via EXAFS spectroscopy as well. In the case of the metallocenes,[103] little is known about the reactions occurring in a biological milieu although hydrolysis reactions analogous to those for *cis*-DDP are known to occur and the loss of the cyclopentadienyl ring has been suggested as a possibility. EXAFS spectroscopy should certainly be able to show whether the chloro ligands are gone and also whether the 10 carbon atoms have been replaced. In the case of the gold complexes, significant changes should be expected in the XANES and EXAFS spectra on binding to a nucleic acid. If the phosphorus is still bound to gold, its signature should be obvious in the XANES spectrum. Gold–nitrogen binding can be detected in fitting the EXAFS spectrum although the particular binding mode (e.g. N1 vs. N7 for adenine) will be undiscernible.

B. Osmium- and Antimony-Based Drugs

Several other metal-based drugs either are in use or have been suggested for therapy. EXAFS studies of these materials and their metabolites may provide information available by no other means. As an example, osmium compounds have been used in the treatment of rheumatoic arthritis.[107] Early work utilized the osmate ion[108] or osmium tetroxide both of which bind irreversibly to the joint causing a "chemical synovectomy". More recently a group at Southern Illinois University[107] investigated the less toxic osmarins, osmium–carbohydrate polymers. As osmium is a basis of electron micrographic stains; its biodistribution with localization of the osmium in the joint was established easily. However, little is known about the biochemistry of these deposits. EXAFS and XANES studies might have several advantages, and the Os L_{III} edge is at 10.870 keV, an energy easily accessible with synchrotron radiation. First, these studies can be conducted on the actual tissues as in the case of the gold deposits called aurosomes.[21] Second, reduction of osmium tetroxide or osmate may well be discernible in the XANES spectrum, and the "yl" type of metal–oxygen double bond may well have a signature in the XANES spectrum. Third, the replacement of a "yl" oxygen with its characteristically very short metal–oxygen bond by other ligands should result in significant changes in the EXAFS spectrum as well.

Another element of interest is antimony. The intriguing history of antimony compounds and their use as drugs is summarized in an entertaining review by McCallum.[2] Although the widest use is in veterinary medicine,[3] the compounds are used to treat parasites in humans as well. A significant advance in the administration of antimonials occurred in 1978 with the demonstrations[109,110] that extremely effective drug delivery was possible with liposomes as drug carriers. The parasite leishmania infects at least 12 million people and is a severe public health problem in tropical and subtropical areas of the world. Leishmania reside chronically in the reticuloendothelial cells; and since those cells phagotize injected liposomes, a vehicle for safe and efficient delivery of the antimonials to the site of the parasite is available. Further work on this method of therapy has been reported;[111] however, rather limited attention has been given to studying the antimony biochemistry itself.

The trivalent organic antimonials are used to treat schistomiasis as well. They are thought to inhibit gly-

colysis, apparently at the phosphofructokinase step;[112] however, little is known of the fate of antimony, and the importance of glycolysis inhibition has been questioned.[113] While X-ray absorption spectra at the L_I and L_{III} edges have been reported for antimony-containing materials,[114] no studies relevant to the antimony-based drugs have been undertaken. EXAFS and XANES studies of these materials should be both easy and informative. In the case of liposomes containing tartar emetic or sodium antimony gluconate, 50% of the antimony was retained after 1 week, the remainder escaping into solution.[110] However, at the site of action, the antimony must be freed to interact chemically with the parasite. Substitution and redox reactions at this site may subsequently be studied by EXAFS and XANES spectroscopy.

C. Other Metals of Importance to Health

Many other metals are of some importance in health-related matters. For instance, ^{67}Ga is used to image soft tumors[115] while rhenium complexes have been suggested both as bone-imaging agents and as palliatives in the case of bone metastases of prostate cancer.[116] Cadmium and mercury are public health threats whose distribution and toxicity have received wide notice.[117-119] Nickel[120,121] and chromium[122,123] carcinogenesis were featured aspects of a Dec 1984 symposium on metal-related toxicity and carcinogenesis. In nearly all of these cases EXAFS and XANES spectroscopy should be able to provide new and unique insight at the molecular level into the biological chemistry of these metals.

V. Additional Structural Information Using Wide-Angle X-ray Scattering (WAXS) and Differential Anomolous Scattering (DAS)

A. WAXS and DAS

A recurring theme throughout this review has been the frequently frustrating inability of EXAFS to reveal neighbors beyond the first coordination shell. EXAFS from a series of gold dimeric complexes synthesized by Fackler and his students[124] failed to reveal gold–gold interactions[28] known from single-crystal X-ray diffraction to include metal–metal distances as small as 3.0 Å. Considered from a background of using gold–gold vectors in a Patterson function to solve crystal structures, this EXAFS "invisibility" is astounding. There are two reasons for the problem: First, as pointed out by Lock and Hitchcock[92] and Teo Averill and Antonio,[56] the back-scattering from a heavy atom will predominate over back-scattering from light atoms only at high values of k. For many samples, especially biologically relevant ones with low absorber concentrations, data obtained at high k are so noisy as to obscure the signal. Second, as pointed out by Kortright, Warburton, and Bienenstock,[125] low-k data contain information weighted toward longer distances. Certainly, small-angle scattering is known to reveal long-range information.[126] However, with EXAFS it is difficult to define the point at which $k = 0$. Also some overlap between EXAFS and XANES regions occurs so most workers discard low-k data, retaining values from $k > 3$ Å^{-1} only.[127]

No such ambiguity exists in X-ray scattering; $k = 0$ at $2\theta = 0°$, where 2θ is the scattering angle. Thus, WAXS offers a means to obtain more long-range information than EXAFS. X-ray diffraction from liquids and amorphous materials was first studied prior to World War II with many of the early studies by Warren[128] and Zernicke and Prins.[129] Studies of this type were used to establish solution structures of heavy-metal polymers, such as the bismuth hydroxide hexamer,[130] long before EXAFS spectra were properly interpreted. One of the principal difficulties with liquid diffraction of X-rays is that the X-ray flux available from X-ray tubes is low and that long times for data collection are necessary, even with extremely concentrated solutions, if structural information is to be successfully extracted. A second difficulty is that X-ray diffraction from liquids is nonselective and gives pair distance information for *every* possible atom pair in the sample weighted by the product of the atomic numbers of the partners and their relative abundance in the sample. With the advent of storage ring sources of X-ray synchrotron radiation, both of these problems may be overcome. The flux available[13] from the wiggler sources at SSRL and recently on the large PEP ring at Stanford operating at 14 GeV is 5–6 orders of magnitude more intense than that previously available. Since the wiggler source provides white radiation, a means is available to solve, at least partially, the second problem mentioned for liquid diffraction, the lack of selectivity. Templeton has shown[131] that at the L_{III} absorption edges for materials such as gold there is an enormous change in anomalous dispersion, with approximately 20 of 80 electrons scattering anomalously near the edge. This suggests that differential anomalous scattering (DAS) can be specific to pair interactions between the heavy atom (gold) of interest and all of its neighbors. Most trivially, if one takes diffraction data using X-rays of energy immediately below the gold L_{III} absorption edge and also measures a second data set for X-rays of energy 100 eV below the edge, the difference between these two must involve diffraction in which a gold atom is one of the diffracting pair. For a change in energy of 100 eV at an energy of nearly 12 keV, essentially no change will occur in scattering by non-gold atoms and the difference data set will have had information depending only on non-gold atoms removed. For gold, the scattering efficiency will have changed a great deal and thus the difference data set will retain gold-centered information.

Although X-ray scattering from amorphous materials was well understood by 1934 with the introduction of a Fourier transform of the data to yield a radial distribution function,[128] the use of differential anomalous scattering is much more recent. One of the principal developers of DAS is Arthur Bienenstock, the director of SSRL. He reviewed the technique in a book chapter on structural studies of amorphous materials.[132] His group in the Applied Physics Department at Stanford has worked largely on glasses and alloys. Our own work,[133] described below, is the first of which we know to use WAXS/DAS for studies of molecular species such as the gold antiarthritis drugs. Also by way of an introduction to this area, in late 1986, R. D. Lorentz and J. E. Penner-Hahn[134] published the results of a solution study of tungsten acetate clusters. A readable intro-

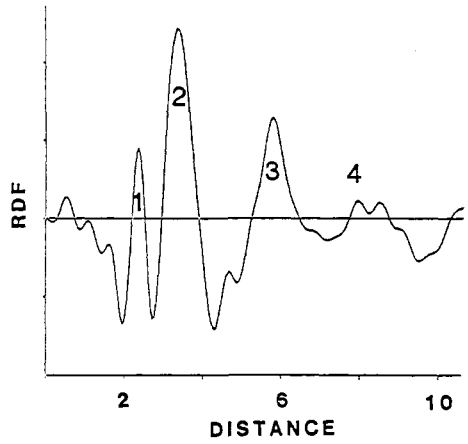

Figure 18. Radial distribution function, with average electron density subtracted out, of sodium gold thiomalate calculated from WAXS data. The peaks at 3.35, 5.8, and 8.1 Å represent gold–gold vectors.

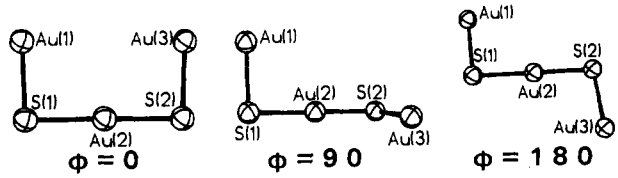

Figure 19. Relationships of Au–Au second nearest neighbors depending on the torsional angle, ϕ, about the line S(1)–Au(2)–S(2).

duction to the WAXS technique can be found in the text by H. P. Klug and L. E. Alexander.[135]

B. Myochrisin and Solganol Structures by WAXS/DAS

Recently we performed two WAX/DAS experiments with Karl Ludwig using the materials diffractometer on wiggler side station IV-3 at the Stanford Synchrotron Radiation Laboratories. One study was on the gold-based drug myochrisin,[133] and the radial distribution function (RDF) obtained from WAXS data measured at 11.915 keV is shown in Figure 18. Long-range information is obtained with the principal peaks at 3.35 and 5.80 Å. Clearly, the RDF reveals extremely important structural information. Note that this is a true RDF; the distances that can be read from the Fourier transform are actual interatomic distances. There are no phase shifts that require distance corrections as in EXAFS spectroscopy. The peak at 2.3 Å corresponds to the gold–sulfur bond, known from our previous EXAFS studies (section IB) to result from two sulfur atoms bound to each gold at 2.30 Å. The peak at 3.35 Å corresponds to a gold–gold distance with a thiolate sulfur bridging the two gold atoms. The bridging angle of Au–S–Au of 94° is in good agreement with the unpublished[136] crystal structure of an analogously bridged gold dimer. More importantly, the peak at 5.8 Å can also be ascribed to a gold–gold interaction if we postulate an oligomer or extended polymer. The second nearest gold–gold interaction depends on the torsional angle ϕ as well as the Au–S–Au (94°) and S–Au–S (180° assumed) angles. The torsional angle ϕ is defined as the angle between the Au(1)–S(1) and S(2)–Au(3) vectors when projected down the S(1)–Au(2)–S(2) vector. The cases for ϕ = 0, 90, and 180° are indicated in Figure 19. The vector Au(1)–Au(3) varies in length, going

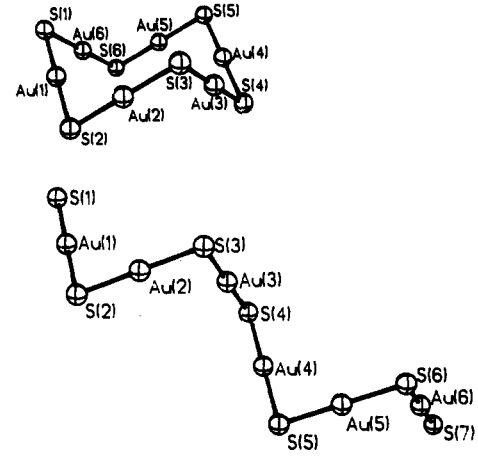

Figure 20. Postulated hexameric $(Au–S)_6$ ring structure of myochrisin (sodium gold(I) thiomalate) and the related but more likely open-chain structure.

from 5.0 Å at ϕ = 0° to 6.7 Å at ϕ = 180°, with a value of 5.8 Å at ϕ = 90°. Thus, the second most major peak in the RDF at 5.8 Å can be ascribed to a Au(1)···Au(3) interaction with ϕ = 90°. The two simplest ways to propagate this chain repeating the ϕ = 90° relation and thus maintaining the Au–Au distance of 5.8 Å are an infinite polymer or a puckered-ring hexamer like the chair form of cyclohexane, with sulfur atoms replacing carbon and the gold atoms midway between adjacent sulfur atoms. Both the cyclic framework and the open-chain structure are illustrated in Figure 20. Remarkably, these two structures may be distinguished based on distance between Au(1) and Au(4). The cyclohexane-like structure predicts Au(1)–Au(4) as 6.7 Å, a position where there is no excess density in the RDF. The open-chain structure turns out from itself, and the distance Au(1)–Au(4) is lengthened to a predicted value of 8.1 Å in agreement with the split peak labeled 4 in the RDF.

We collected data on myochrisin both as a mull and as a concentrated solution. The data from solution samples show similar RDF's to those obtained from mulls, indicating that the gold–gold interactions are intramolecular rather than between molecules and that the chain structure persists in solution. The open-chain structure shown in Figure 20 requires an "extra" thiomalate to provide an end cap. For a hexamer this requires seven thiomalate ligands, in remarkable agreement with previous findings that the drugs as formulated contain roughly 15% "excess" ligand relative to the expected one-to-one formulation.[137] Given an open-chain structure there is no reason to expect all chains to be hexamers. Rather it is likely that 6 represents an average polymerization number only.

We also examined the drug solganol (gold thioglucose) using WAXS and DAS techniques. The differential distribution function (DDF) computed from the Solganol data is given in Figure 21. This function computed from the difference between data measured at 11.918 and 11.800 keV is nominally a gold-based radial distribution function. Two obvious points from the DDF are, first, there is a peak at an impossibly short distance, 0.5 Å, and, second, there is long-range information in the DDF, with three Au–Au distances of 3.37, 6.0, and 9.1 Å. The peak at 0.5 Å, we believe, results from errors in the normalization of the data and is much

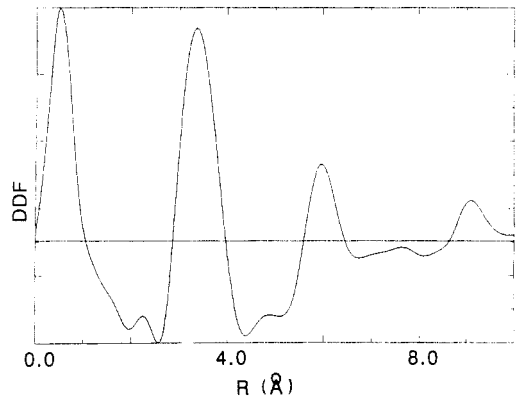

Figure 21. Differential distributin function (DDF) for solganol (gold thioglucose) showing slightly longer Au(1)···Au(3) and Au(1)···Au(4) distances than those for myochrisin.

exaggerated due to the taking of differences. The peak at 3.35 Å is in agreement with that from myochrisin and represents the Au(1)···Au(2) distance with an Au(1)–S(2) distance of 2.30 Å and an Au(1)–S(2)–Au(2) angle of 94° in complete agreement with the myochrisin gold bond lengths and angles as well as sulfur bond lengths and angles. The difference comes in the peak at 6.0 Å for solganol as opposed to 5.8 Å for myochrisin. The larger distance in solganol results from a more open torsional angle, ϕ, of 104°. Thus, both of these drugs have nearly identical frameworks and differ only in conformational detail. The import of these experiments is considerable. First, they unequivocally show that these gold-based antiarthritis drugs are polymeric and strongly suggest they are open-chain structures. Second, they show that WAXS/DAS experiments can provide extremely useful information not available from EXAFS studies and that these experiments can be performed on biologically relevant samples such as aqueous drug solutions.

C. Advantages and Limitations of WAXS and DAS

Clearly these techniques provide new possibilities of obtaining long-distance information, and there are several cases already cited in this review where such information would be extremely helpful. Whether gold thionein utilizes bridging by cysteine sulfur atoms to form gold clusters, whether the zinc and cadmium is metallothionein interact with gold atoms in the case of partial substitution, what the relations between technetium and tin atoms are in various imaging agents, whether diphosphonate ligands form technetium polymers, and whether they bridge to calcium on bone surface are all now being examined in our laboratory.

There are some severe limitations to these techniques that should be addressed. First, scattering is a low-probability process, and thus the signal is quite weak. Second, differential anomalous scattering relies on the difference between two weak signals for its information, and thus suffers from high noise levels. The earliest liquid diffraction work was done on pure atomic substances such as mercury and argon. When more than one atomic type is present, interpretation of data is more difficult. Generally the best cases will involve heavy-atom to heavy-atom interaction and materials need to contain a few percent of the atoms of interest. In the first applications sample size was large (ca. 1.0 g), but recently we have successfully measured acceptable data in a transmission scattering experiment from as little as 8 mg of myochrisin. In the DAS experiment, both for wavelength tunability and for the high flux needed to improve counting statistics, a synchrotron source is a necessity; however, a WAXS experiment can be performed with an X-ray tube source given sufficiently long counting times. The joint areas of WAXS and DAS are complementary to EXAFS and coupled with that technique offer interesting new possibilities for structure determination.

VI. Acknowledgment

Much of our work described here was performed under the sponsorship of National Science Foundation Grants PCM8023743 and PCM8402651. Recent work has been supported by the National Institutes of Health Grant GM35404. All of our experiments and some by others described here were performed at the Stanford Synchrotron Radiation Laboratories, which were originally supported by NSF and are now supported by the Department of Energy. We thank our collaborators Professors K. G. Tepperman, E. Deutsch, and C. F. Shaw; Drs. Jon Doi, M. J. Heeg, K. Ludwig, and D. T. Hill; and John Watkins. We also thank Professors J. P. Fackler, R. A. Scott, C. J. Lock, R. Bau, E. D. Crozier, and A. Bienenstock for copies of their papers prior to publication.

VII. References

(1) Sutton, B. M. In *Platinum, Gold, and Other Metal Chemotherapeutic Agents*; Lippard, S. J., Ed.; ACS Symposium Series 209; American Chemical Society: Washington, DC, 1983; pp 355–369.
(2) McCallum, R. I. *Proc. R. Soc. Med.* **1977**, *70*, 756.
(3) Windholz, M., Ed. *Merck Index*, 10th ed.; Merck: Rahway, NJ, 1983; p 839.
(4) Chandler, J. W.; Rotkis, W. M. In *Clinical Ophthamology*; Duane, T. D., Ed.; Harper and Row: Philadelphia, 1983; Vol. 4, Chapter 6, p 2.
(5) Empire Rheumatism Council *Ann. Rheum. Dis.* **1961**, *20*, 315.
(6) Newlands, E. S.; Rustin, G. J. S.; Begent, R. H. J.; Parker, D.; Bagshawe, K. D. *Lancet* **1983**, *1*(8331), 948.
(7) Deutsch, E.; Libson, K.; Jurisson, S.; Lindoy, L. F. *Prog. Inorg. Chem.* **1983**, *30*, 75.
(8) Pinto, A. L.; Naser, L. J.; Essigmann, J. M.; Lippard, S. J. *J. Am. Chem. Soc.* **1986**, *108*, 7405.
(9) Pinkerton, T. C.; Heineman, W. R.; Deutsch, E. *Anal. Chem.* **1980**, *52*, 1106.
(10) Krull, I. S.; Ding, X.-D.; Braverman, S.; Selavka, C.; Hochberg, F.; Sternson, L. A. *J. Chromatogr. Sci.* **1983**, *21*, 166.
(11) Razi, M. T.; Otiko, G.; Sadler, P. J. *ACS Symp. Ser.* **1983**, *No. 209*, 371.
(12) Sayers, D. E.; Stern, E. A.; Lytle, F. W. *Phys. Rev. Lett.* **1971**, *27*, 1204.
(13) Winick, H. In *Synchrotron Radiation Research*; Winick, H., Doniach, S., Eds.; Plenum: New York, 1980; p 27.
(14) Cramer, S. P.; Hodgson, K. O. *Prog. Inorg. Chem.* **1979**, *25*, 1.
(15) Scott, R. A. *Methods Enzymol.* **1985**, *117*, 414.
(16) Teo, B. K. In *EXAFS Spectroscopy*; Teo, B. K., Joy, D. C., Eds.; Plenum: New York, 1981; p 13.
(17) Brown, D. H.; Smith, W. E. *Chem. Soc. Rev.* **1980**, *9*, 217.
(18) Shaw, C. F., III *Inorg. Perspect. Biol. Med.* **1979**, *2*, 287.
(19) Lorber, A.; Simon, T. M. *Gold Bull.* **1979**, *12*, 149.
(20) Rae, K. J.; Mackay, C. N. N.; McNeil, C. J.; Brown, D. H.; Smith, W. E.; Lewis, D.; Capell, H. A. *Ann. Rheum. Dis.* **1986**, *45*, 839.
(21) Ghadially, F. N. *J. Rheum.* **1979**, *6* (Suppl. 5), 45.
(22) Lewis, A. J.; Walz, D. T. *Prog. Med. Chem.* **1982**, *19*, 1.
(23) Gold as Au(II) and also as Au(V) has been demonstrated;[24-26] however, neither oxidation state seems likely to occur in a biological milieu.
(24) Porter, L. C.; Fackler, J. P., Jr. *Acta Crystallogr., Sect. C: Cryst. Struct. Commun.* **1986**, *C42*, 1646.
(25) Porter, L. C.; Fackler, J. P., Jr. *Acta Crystallogr., Sect. C: Cryst. Struct. Commun.* **1986**, *C42*, 1128.

(26) Puddephat, R. J. *The Chemistry of Gold*; Elsevier: New York, 1978; p 96.
(27) Elder, R. C.; Eidsness, M. K.; Heeg, M. J.; Tepperman, K. G.; Shaw, C. F., III; Schaeffer, N. In *Platinum, Gold, and Other Metal Chemotherapeutic Agents*; Lippard, S. J., Ed.; ACS Symposium Series 209; American Chemical Society: Washington, DC, 1983; pp 385–400.
(28) Eidsness, M. K. Ph.D. Thesis, University of Cincinnati, 1984.
(29) Hill, D. T.; Sutton, B. M. *Cryst. Struct. Commun.* **1980**, *9*, 679.
(30) Sadler, P. J. *Struct. Bonding (Berlin)* **1976**, *29*, 171.
(31) Shaw, C. F.; Schmitz, G.; Thompson, H. O.; Witkiewicz, P. *J. Inorg. Biochem.* **1979**, *10*, 317.
(32) Mazid, M. A.; Razi, M. T.; Sadler, P. J.; Greaves, G. N.; Gurman, S. J.; Koch, M. H. J.; Phillips, J. C. *J. Chem. Soc., Chem. Commun.* **1980**, 1261.
(33) Ruben, H.; Zalkin, A.; Faltens, M. O.; Templeton, D. H. *Inorg. Chem.* **1974**, *13*, 1836.
(34) Gerber, D. A. *J. Pharmacol. Exp. Ther.* **1964**, *143*, 137.
(35) Jellum, E.; Munthe, E.; Guldal, G.; Aaseth, J. *Scand. J. Rheum.* **1979**, Suppl. 28, 28.
(36) Coffer, M. T.; Shaw, C. F., III; Eidsness, M. K.; Watkins, J. W., II; Elder, R. C. *Inorg. Chem.* **1986**, *25*, 333.
(37) Tepperman, K.; Finer, R.; Donovan, S.; Elder, R. C.; Doi, J.; Ratliff, D.; Ng, K. *Science (Washington, D.C.)* **1984**, *225*, 430.
(38) Shaw, C. F., III; Schaeffer, N. A.; Elder, R. C.; Eidsness, M. K.; Trooster, J. M.; Calis, G. H. M. *J. Am. Chem. Soc.* **1984**, *106*, 3511.
(39) Otvos, J. D.; Armitage, I. M. *Proc. Natl. Acad. Sci. U.S.A.* **1980**, *77*, 7094.
(40) Otvos, J. D.; Armitage, I. M. *J. Am. Chem. Soc.* **1979**, *101*, 7734.
(41) Sadler, P. J.; Bakka, A.; Beynon, P. J. *FEBS Lett.* **1978**, *94*, 315.
(42) Garner, C. D.; Hasnain, S. S.; Bremner, I.; Bordas, J. *J. Inorg. Biochem.* **1982**, *16*, 253.
(43) Furey, W. F.; Robbins, A. H.; Clancy, L. L.; Winge, D. R.; Wang, B. C.; Stout, C. D. *Science (Washington, D.C.)* **1986**, *231*, 704.
(44) Laib, J. E.; Shaw, C. F., III; Petering, D. H.; Eidsness, M. K.; Elder, R. C.; Garvey, J. S. *Biochemistry* **1985**, *24*, 1977.
(45) George, G. N.; Winge, D.; Stout, C. D.; Cramer, S. P. *J. Inorg. Biochem.* **1986**, *27*, 213.
(46) Intoccia, A. P.; Flanagan, T. L.; Walz, D. T.; Gutzait, L.; Swagzdis, J. E.; Flagiello, J., Jr.; Hwang, B. Y.-H.; Dewey, R. H.; Noguchi, H. *J. Rheumatol.* **1982**, *9* (Suppl. 8), 90.
(47) Watkins, J. W., II; Elder, R. C.; Greene, B.; Darnall, D. W. *Inorg. Chem.* **1987**, *26*, 1147.
(48) Deutsch, E.; Libson, K. *Comments Inorg. Chem.* **1984**, *3*, 83.
(49) Technetium-99m Generators, Chemistry and Preparation of Radiopharmaceuticals: *Int. J. Appl. Radiat. Isot.* **1982**, *33*, 793. An entire journal issue containing 21 papers on this subject.
(50) Deutsch, E., Nicolini, M., Wagner, H. N., Jr., Eds. *Technetium in Chemistry and Nuclear Medicine*; Cortino International: Verona, Italy, 1983. Distributed by Raven, New York.
(51) Vanderheyden, J.-L.; Libson, K.; Nosco, D. L.; Ketring, A. R.; Deutsch, E. *Int. J. Appl. Radiat. Isot.* **1983**, *34*, 1611.
(52) Tullius, T. D.; Gillum, W. O.; Carlson, R. M. K.; Hodgson, K. O. *J. Am. Chem. Soc.* **1980**, *102*, 5670.
(53) Bandoli, G.; Mazzi, U.; Roncari, E.; Deutsch, E. *Coord. Chem. Rev.* **1982**, *44*, 191.
(54) Teo, B. K.; Lee, P. A. *J. Am. Chem. Soc.* **1979**, *101*, 2815.
(55) Pauling, L. *The Nature of the Chemical Bond*, 3rd ed.; Cornell University: Ithaca, NY, 1960; p 511.
(56) Antonio, M. R.; Teo, B. K.; Averill, B. A. *J. Am. Chem. Soc.* **1985**, *107*, 3583.
(57) Thomas, R. W.; Heeg, M. J.; Elder, R. C.; Deutsch, E. *Inorg. Chem.* **1985**, *24*, 1472.
(58) Thomas, R. W.; Estes, G. W.; Elder, R. C.; Deutsch, E. *J. Am. Chem. Soc.* **1979**, *101*, 4581.
(59) Cotton, F. A.; Davison, A.; Day, V. W.; Gage, L. D.; Trop, H. S. *Inorg. Chem.* **1979**, *18*, 3024.
(60) Garner, C. D.; Hill, L. H.; Mabbs, F. E.; McFadden, D. L.; McPhail, A. T. *J. Chem. Soc., Dalton Trans.* **1977**, 853.
(61) Tkachev, V. V.; Krasochka, O. N.; Atovmyan, L. O. *Zh. Strukt. Khim.* **1976**, *17*, 940.
(62) Bino, A.; Cotton, F. A. *Inorg. Chem.* **1979**, *18*, 2710.
(63) Abrams, M. J.; Davison, A.; Jones, A. G.; Costello, C. E.; Pang, H. *Inorg. Chem.* **1983**, *22*, 2798.
(64) Jones, A. G.; Davison, A.; Abrams, M. J.; Brodack, J. W.; Kassis, A. I.; Goldhaber, S. Z.; Holman, B. L.; Stemp, L.; Manning, T.; Hechtman, H. B. *J. Nucl. Med.* **1982**, *23*, 16.
(65) Gerundini, P.; Savi, A.; Gilardi, M. C.; Margonato, A.; Vicedomini, G.; Zecca, L.; Hirth, W.; Libson, K.; Bhatia, J. C.; Fazio, F.; Deutsch, E. *J. Nucl. Med.* **1986**, *27*, 409. Holman, B. L.; Sporn, V.; Jones, A. G.; Sia, S. T. B.; Perez-Balino, N.; Davison, A.; Lister-James, J.; Kronauge, J. F.; Mitta, A. E. A.; Camin, L. L.; Campbell, S.; Williams, S. J.; Carpenter, A. T. *J. Nucl. Med.* **1987**, *28*, 13.
(66) Vanderheyden, J.-L.; Ketring, A. R.; Libson, K.; Heeg, M. J.; Roecker, L.; Motz, P.; Whittle, R.; Elder, R. C.; Deutsch, E. *Inorg. Chem.* **1984**, *23*, 3184.
(67) Subramanian, V., E. I. du Pont de Nemours and Co., private communication.
(68) Martin, J. L. Ph.D. Thesis, University of Cincinnati, 1987.
(69) Rahman, A. F. M. M.; Elder, R. C.; Libson, K.; Deutsch, E., in preparation.
(70) Tofe, A. J.; Francis, M. D. *J. Nucl. Med.* **1974**, *15*, 69.
(71) Deutsch, E.; Elder, R. C.; Lange, B. A.; Vaal, M. J.; Lay, D. G. *Proc. Natl. Acad. Sci. U.S.A.* **1976**, *73*, 4287.
(72) Cramer, S. P.; Hodgson, K. O.; Gillum, W. O.; Mortenson, L. E. *J. Am. Chem. Soc.* **1978**, *100*, 3398.
(73) Eidsness, M. K.; Flank, A. M.; Smith, B. E.; Flood, A. C.; Garner, C. D.; Cramer, S. P. *J. Am. Chem. Soc.* **1986**, *108*, 2746. Scott, R. A.; Schwartz, J. R.; Cramer, S. P. In *EXAFS and Near Edge Structure*; Hodgson, K. O., Hedman, B., Penner-Hahn, J. E., Eds.; Springer: Berlin, 1984; Vol. 3, p 111.
(74) Libson, K.; Deutsch, E.; Barnett, B. L. *J. Am. Chem. Soc.* **1980**, *102*, 2476.
(75) Elder, R. C.; Rahman, A. F. M. M.; Siddiqui, K. F.; Libson, K.; Deutsch, E., manuscript in preparation.
(76) Creaser, I. I.; Harrowfield, J. M.; Herlt, A. J.; Sargeson, A. M.; Springborg, J.; Geue, R. J.; Snow, M. R. *J. Am. Chem. Soc.* **1977**, *99*, 3181.
(77) Rosenberg, B.; VanCamp, L.; Trosko, J. E.; Mansour, V. H. *Nature (London)* **1969**, *222*, 385.
(78) Carter, S. K. In *Platinum Coordination Complexes in Cancer Chemotherapy*; Hacker, M. P.; Douple, B.; Krahoff, I. H., Eds.; Martinus Nijhoff: Boston, 1984; p 359.
(79) Rosenberg, B. In *Inorganic Chemistry in Biology and Medicine*; Martell, A. E., Ed.; ACS Symposium Series 140; American Chemical Society: Washington, DC, 1980; p 143.
(80) Sherman, S. E.; Gibson, D.; Wang, A. H.; Lippard, S. J. *Science (Washington, D.C.)* **1985**, *230*, 412.
(81) Ciccarelli, R. B.; Solomon, M. J.; Varshavsky, A.; Lippard, S. J. *Biochemistry* **1985**, *24*, 7533.
(82) Lippard, S. J. *Science (Washington, D.C.)* **1982**, *218*, 1075.
(83) Barton, J. K.; Rabinowitz, H. N.; Szalda, D. J.; Lippard, S. J. *J. Am. Chem. Soc.* **1977**, *99*, 2827.
(84) Faggiani, R.; Lippert, B.; Lock, C. J. L.; Rosenberg, B. *J. Am. Chem. Soc.* **1977**, *99*, 777.
(85) Lippert, B.; Lock, C. J. L.; Rosenberg, B.; Zvagulis, M. *Inorg. Chem.* **1978**, *17*, 2971.
(86) Faggiani, R.; Lippert, B.; Lock, C. J. L.; Rosenberg, B. *Inorg. Chem.* **1977**, *16*, 1192.
(87) Faggiani, R.; Lippert, B.; Lock, C. J. L.; Rosenberg, B. *Inorg. Chem.* **1978**, *17*, 1941.
(88) Teo, B. K.; Kijima, K.; Bau, R. *J. Am. Chem. Soc.* **1978**, *100*, 621.
(89) Teo, B. K.; Eisenberger, P.; Reed, J.; Barton, J. K.; Lippard, S. J. *J. Am. Chem. Soc.* **1978**, *100*, 3225.
(90) Hitchcock, A. P.; Lock, C. J. L.; Pratt, W. M. C. *Inorg. Chim. Acta* **1982**, *66*, L45.
(91) Speranyini, R. A. Ph.D. Thesis, McMaster University, 1980. Quoted in ref 90.
(92) Hitchcock, A. P.; Lock, C. J. L.; Pratt, W. M. C.; Lippert, B. In *Platinum, Gold, and Other Metal Chemotherapeutic Agents*; Lippard, S. J., Ed.; ACS Symposium Series 209; American Chemical Society: Washington, DC, 1983; p 209.
(93) Hitchcock, A. P.; Martins, M. L.; Lock, C. J. L. In *Platinum Coordination Complexes in Cancer Chemotherapy*; Hacker, M. P., Douple, E. B., Krakoff, I. H., Eds.; Martinus Nijhoff: Boston, 1984; p 62.
(94) Hitchcock, A. P.; Lock, C. J. L.; Lippert, B. *Inorg. Chim. Acta* **1986**, *124*, 101.
(95) Howe-Grant, M.; Lippard, S. J. *Metal Ions in Biological Systems*; Siegel, H., Ed.; Marcel Dekker: New York, 1980; Vol. 11, p 63.
(96) Bruck, M. A.; Korte, H.-J.; Bau, R.; Hadjiliadis, N.; Teo, B. K. In *Platinum, Gold, and Other Metal Chemotherapeutic Agents*; Lippard, S. J., Ed.; ACS Symposium Series 209; American Chemical Society: Washington, DC, 1983; pp 245–262.
(97) Heitner, H. I.; Lippard, S. J. *Inorg. Chem.* **1974**, *13*, 815.
(98) Heitner, H. I.; Lippard, S. J.; Sunshine, H. R. *J. Am. Chem. Soc.* **1972**, *94*, 8936.

(99) Bruck, M. Ph.D. Thesis, University of Southern California, 1983.
(100) Bau, R., private communication.
(101) Clarke, M. J. In *Metal Ions in Biological Systems*; Siegel, H., Ed.; Marcel Dekker: New York, 1980; Vol. 11, p 231.
(102) Cleare, M. J.; Hydes, P. C. In *Metal Ions in Biological Systems*; Siegel, H., Ed.; Marcel Dekker: New York, 1980; Vol. 11, p 30.
(103) Kopf, H.; Kopf-Maier, P. In *Platinum, Gold, and Other Metal Chemotherapeutic Agents*; Lippard, S. J.; Ed.; ACS Symposium Series 209; American Chemical Society: Washington, DC, 1983; p 315.
(104) Alberding, N.; Farrel, N.; Crozier, E. D. *J. Am. Chem. Soc.* **1985**, *107*, 384.
(105) Simon, T. M.; Kunishima, D. H.; Vibert, G. J.; Lorber, A. *Cancer* **1979**, *44*, 1965.
(106) Mirabelli, C. K.; Johnson, R. K.; Hill, D. T.; Faucette, L. F.; Girard, G. R.; Kuo, G. Y.; Sung, C. M.; Crooke, S. T. *J. Med. Chem.* **1986**, *29*, 218.
(107) Hinckley, C. C.; Bemiller, J. N.; Strack, L. E.; Russell, L. D. In *Platinum, Gold, and Other Metal Chemotherapeutic Agents*; Lippard, S. J., Ed.; ACS Symposium Series 209; American Chemical Society: Washington, DC, 1983; p 421.
(108) Birch, N. J.; Sadler, P. J. In *Inorganic Biochemistry*; Hill, H. A. O., Ed.; Royal Society of Chemistry: London, 1981; Vol. 2, p 346.
(109) Alving, C. R.; Steck, E. A.; Chapman, W. L.; Waits, V. B.; Hendricks, L. D.; Swartz, G. M.; Hanson, W. L. *Proc. Natl. Acad. Sci. U.S.A.* **1978**, *75*, 2959.
(110) New, R. R. C.; Chance, M. L.; Thomas, S. C.; Peters, W. *Nature (London)* **1978**, *272*, 55.
(111) Rao, L. S. *J. Parenter. Sci. Technol.* **1983**, *37*, 72.
(112) Shapiro, T. A.; Talalay, P. *Exp. Parisitol.* **1982**, *54*, 379.
(113) Motram, J. C.; Combs, G. H. *Exp. Parisitol.* **1985**, *59*, 151.
(114) Dalba, G.; Fornasini, P.; Burattini, E. *J. Phys. C* **1983**, *16*, L1091.
(115) Hayes, R. L. In *Recent Advances in Nuclear Medicine*; Lawrence, J. H., Winchell, S., Eds.; Grune and Stratton: New York, 1983; Vol. 6, p 177.
(116) Weininger, J.; Ketring, A. R.; Deutsch, E. A. *Nuklearmedizin* **1984**, *23*, 81.
(117) Birch, N. J.; Sadler, P. J. In *Inorganic Biochemistry*; Hill, H. A. O., Ed.; Royal Society of Chemistry: London, 1980; Vol. 1, p 356.
(118) Tanaka, K.; Onosaka, S.; Min, K.-S.; Fukuhara, C. *Abstracts of Papers*, International Chemical Congress of Pacific Basin Societies, Honolulu, HI; American Chemical Society: Washington, DC, 1984; Abstract 04B13.
(119) Rabenstein, D. L. *Abstracts of Papers*, International Chemical Congress of Pacific Basin Societies, Honolulu, HI; American Chemical Society: Washington, DC, 1984; Abstract 04B14.
(120) Sarkar, B. *Abstracts of Papers*, International Chemical Congress of Pacific Basin Societies, Honolulu, HI; American Chemical Society: Washington, DC, 1984; Abstract 04B11.
(121) Costa, M. *Abstracts of Papers*, International Chemical Congress of Pacific Basin Societies, Honolulu, HI; American Chemical Society: Washington, DC, 1984; Abstract 04B18.
(122) Wetterhahn, K.; Cupo, D. Y. *Abstracts of Papers*, International Chemical Congress of Pacific Basin Societies, Honolulu, HI; American Chemical Society: Washington, DC, 1984; Abstract 04B16.
(123) Osterberg, R.; Persson, D.; Bjursell, G. *Abstracts of Papers*, International Chemical Congress of Pacific Basin Societies, Honolulu, HI; American Chemical Society: Washington, DC, 1984; Abstract 04B17.
(124) Mazany, A. M.; Fackler, J. P., Jr. *J. Am. Chem. Soc.* **1984**, *106*, 801.
(125) Kortright, J.; Warburton, W.; Bienenstock, A. In *EXAFS and Near Edge Structure*; Bianconi, A., Inoccia, L., Stipcich, S., Eds.; Springer: Berlin, 1983, Vol. 2, p 362.
(126) Klug, H. P.; Alexander, L. E. *X-ray Diffraction Procedures for Polycrystalline and Amorphous Materials*; Wiley: New York, 1954; p 635.
(127) Scott, R. A. In *Physical Techniques in Biological Research*; Rosseau, D., Ed.; Academic: New York, 1983; Vol. 2.
(128) Warren, B. E.; Gingrich, N. S. *Phys. Rev.* **1934**, *46*, 368.
(129) Zernicke, F.; Prins, J. A. *Z. Phys.* **1927**, *41*, 184.
(130) Levy, H. A.; Danford, M. D.; Agron, P. A. *J. Chem. Phys.* **1959**, *31*, 1458.
(131) Templeton, L. K.; Templeton, D. H.; Phizackerley, R. P. *J. Am. Chem. Soc.* **1980**, *102*, 1185.
(132) Bienenstock, A. In *Physical Properties of Amorphous Materials*; Adler, D., Schwartz, B. B., Steele, M. C.; Eds.; Plenum: New York, 1985; p 171.
(133) Elder, R. C.; Ludwig, K.; Cooper, J. N.; Eidsness, M. K. *J. Am. Chem. Soc.* **1985**, *107*, 5024.
(134) Lorentz, R. D.; Bino, A.; Penner-Hahn, J. E. *J. Am. Chem. Soc.* **1986**, *108*, 8116.
(135) Klug, H. P.; Alexander, L. E. *X-ray Diffraction Procedures for Polycrystalline and Amorphous Materials*; Wiley: New York, 1954; p 586.
(136) Hill, D. T.; Gustke, K.; Heeg, M. J.; Elder, R. C., unpublished work.
(137) Rudge, S. R.; Perrett, D.; Swannell, A. J.; Drury, P. L. *J. Rheumatol.* **1984**, *11*, 150.